



The University of  
**Nottingham**

# **CIVIL MARITIME GNSS COMBINATIONS IN ARCTIC AREAS**

**By**

**Henning Sulen**

Project thesis submitted to the University of Nottingham in partial fulfilment of the  
degree of Master of Science in Positioning and Navigational Technology

August 2015

**Supervisor: Dr Xiaolin Meng**

**Department of Civil Engineering, The University of Nottingham, UK**

## **PLAGIARISM STATEMENT**

This is to confirm that the content of this thesis is my own work and does not break the University, Department or module conventions on plagiarism as outlined in the Department of Civil Engineering MSc Civil Engineering Postgraduate Handbook.

Date:

\_\_\_\_\_

**Signed**

## **ABSTRACT**

*GPS is the most used GNSS system on board civilian vessels using civil GPS signal L1 only. Since 2011, there have been two fully operational GNSS systems – GPS since 1995 and GLONASS since 2011. Both GPS and GLONASS conduct modernization programs involving new satellites, new signals and new ground segment stations. New GNSS equipment is needed to exploit the new signals and both GNSS systems in a combined positioning approach. Future GNSS systems are Galileo and BeiDou.*

*The Northeast Passage (NEP) is the shipping route between Europe and Asia passing Norwegian and Russian territory. The NEP is about 40% shorter than the voyage through Suez channel. The reduction of sea ice in the arctic area around Svalbard and NEP has increased the use of NEP for civilian vessels. The cold and harsh environment in NEP demands robust and reliable navigation equipment for solving position solutions. The distinctiveness of the Arctic is the latitude. It is higher than the inclination angle to Equator of the GNSS satellites orbital planes and the arctic area has ionospheric irregularities due to Aurora Borealis.*

*In the thesis, a GNSS measurement was conducted at Svalbard on 16 to 18 June 2015. The aim of the research is to compare the GNSS combinations positioning approach: GPS Single, GLONASS, GPS Dual, GPS+GLONASS combined and DGPS.*

*The RTKLIB version 2.4.3, an open source GNSS processing software program was used to evaluate the solutions of the GNSS combinations by post-processing the data collected at Svalbard. The research compared the GNSS combinations in a long and short static test, in a dynamic ship moving simulation and during sun activity.*

*The GPS+GLONASS combination has shown to be more robust in accuracy, precision, availability of all GNSS satellites and their signals during the static and dynamic test in the Arctic. Due to redundancy and robustness, it is advantageous to use the GPS+GLONASS combination for safe navigation in the arctic area around Svalbard and in the Northeast Passage for civilian vessels.*

## **ACKNOWLEDGMENT**

I want to express my gratitude to all who have been involved in this MSc thesis.

Thanks to the Royal Norwegian Navy for the scholarship and financial support of the research.

To make the fieldwork possible I want to thank Ole Petter Storstad for approving my application to conduct the measurement at KSAT Svalbard Satellite Station and Kjetil Slettnes for all assistance and transport during the stay.

Thanks to my colleagues for constructive discussion and to Anne Linda Løhre for looking at my English.

Thanks to technician Sean Ince for teaching me the Leica equipment and help during the test measurements.

A warm thanks to Dr Lukasz Bonenberg for acquiring the Manfrotto tilt head and the screw transitions and for constructive discussions about the research. Also thank you for giving guidance about where I can find the answers instead of just answering my questions.

A warm thanks to my supervisor Dr Xiaolin Meng for your eagerness, helpfulness, guidance and helpful feedback.

Thanks to my son Brage for keeping me on the edge.

A special thanks to my daughters Sunniva and Silje who joined me here in Nottingham. You took up the challenge by one year at the English school Dagfa without speaking English leaving your friends behind in Norway. Your courage and zest for life inspires me.

Finally, I wish to thank my wife Ramona for taking the challenge of staying one year in Nottingham, putting your artist career on hold and leaving your artist environment to support our daughters and me. I am very grateful for your help and understanding through the whole year and during the writing of this thesis. It had been impossible without you.

Nottingham 27 August 2015

Henning Sulen

## TABLE OF CONTENT

PLAGIARISM STATEMENT .....	1
ABSTRACT .....	2
ACKNOWLEDGMENT.....	3
LIST OF FIGURES .....	7
LIST OF TABLES AND DIAGRAMS.....	9
LIST OF ABBREVIATIONS .....	10
1 INTRODUCTION .....	13
1.1 Background .....	13
1.2 Aims And Objectives Of The Research .....	15
1.2.1 Hypothesis .....	15
1.2.2 Aim of the Research .....	16
1.2.3 Objectives of the Research .....	16
1.2.4 Thesis Outline.....	16
2 LITERATURE REVIEW .....	18
2.1 Global Navigational Satellite Systems (GNSS).....	18
2.2 The Signal Structure Of Global Positioning System (GPS) .....	19
2.2.1 GPS Carrier Wave – Component One .....	19
2.2.2 Ranging Code – Component Two.....	20
2.2.3 Navigation Data Message – Component Three.....	20
2.2.4 Modulation - Ranging Code and Navigation Data .....	20
2.2.5 Code Diversion Multiple Access (CDMA).....	22
2.2.6 Direct Sequence Spread Spectrum (DS-SS).....	22
2.2.7 Signal Power.....	23
2.2.8 Signal to Noise Ratio .....	23
2.2.9 Operational GPS Satellites – Status at 9 August 2015 .....	24
2.3 The Signal Structure Of GLONASS .....	25
2.3.1 GLONASS Satellite Signals.....	26
2.3.2 Frequency Diversion Multiple Access (FDMA) .....	27
2.3.3 Operational GLONASS Satellites – Status at 9 August 2015 .....	27
2.4 GLONASS And GPS Comparison .....	28
2.5 GNSS System Biases And Errors.....	32
2.5.1 Satellite Ephemeris Errors .....	32
2.5.2 Satellite Clock Error.....	32

2.5.3	Ionospheric Bias .....	32
2.5.4	Tropospheric Bias.....	34
2.5.5	Multipath.....	34
2.5.6	Receiver Errors .....	35
2.6	GNSS Satellite Constellation Geometry.....	35
2.6.1	DOP.....	35
2.7	GNSS System Vulnerability .....	37
2.7.1	Unintentional Interference.....	38
2.7.2	Intentional Interference .....	39
2.8	GNSS Positioning Approaches .....	40
2.8.1	Principle of Stand Alone Pseudo Range Positioning.....	40
2.8.2	Stand Alone Pseudo Ranges.....	40
2.8.3	Differential GPS .....	45
2.9	RTKLIB 2.4.3. ....	45
3	METHODOLOGY.....	47
3.1	Equipment.....	47
3.2	Test Measurement.....	48
3.3	GNSS Combinations.....	49
3.4	Data Recording .....	49
3.4.1	Data Recording Times .....	49
3.4.2	Data Recording Files .....	50
3.5	Static Receiver.....	51
3.5.1	Long Period .....	51
3.5.2	Short Period .....	52
3.6	Ship Movement Simulation .....	52
3.6.1	Ship Movement Cycle .....	53
3.6.2	Ship Movement Procedure .....	54
3.6.3	Ship Movement Cycle Times .....	55
3.7	Sun Activity .....	55
3.8	Data Analysis Techniques .....	56
3.8.1	GNSS Planning Software Tool .....	56
3.8.2	RINEX Raw Data Extraction .....	56
3.8.3	Data Analysis Software Tool .....	56
3.9	Location Of The Site .....	57
3.9.1	Determination of Site.....	57

3.9.2	True Position of Rover and Base Station .....	59
3.10	Presentation Of Results .....	62
3.11	Research Design Issues And Limitations .....	63
4	RESULTS AND DISCUSSION .....	65
4.1	True Position Of Rover And Base Station .....	65
4.2	Long Period .....	67
4.2.1	Accuracy and Precision.....	67
4.2.2	Signal-to-Noise-Ratio.....	76
4.2.3	Skyplot .....	78
4.2.4	DOP.....	81
4.3	Short Period .....	82
4.3.1	Accuracy and Precision.....	82
4.3.2	DOP and Number of Satellites .....	85
4.3.3	Robustness and Redundancy .....	87
4.4	Ship Movement Simulation .....	88
4.4.1	Multipath Tilt Cycle 2B .....	88
4.4.2	Accuracy and Precision.....	93
4.5	Sun Activity NYA1.....	99
5	CONCLUSION.....	102
6	RECOMMENDATIONS .....	103
	REFERENCES .....	104
	Appendix A: Specifications Leica GS10 .....	108
	Appendix B: Specifications Trimble NETR8 .....	109

## LIST OF FIGURES

Figure 1.1: Map of the Norwegian and Russian arctic coasts.....	13
Figure 2.1: BPSK modulation of a carrier.....	21
Figure 2.2: Each GPS satellite transmitted three Binary Phase Shift Keying.....	21
Figure 2.3: Power spectra of signals transmitted by a GPS satellite.....	21
Figure 2.4: Type and status of GPS satellites at 9 August 2015.....	25
Figure 2.5: Power spectra of signals transmitted by GLONASS satellites.....	26
Figure 2.6: Power spectra of signals of both GPS and GLONASS.....	27
Figure 2.7: The accuracy of GLONASS compared to GPS.....	29
Figure 2.8: Illustrating DOP.....	36
Figure 3.1: Photo at Svalbard of the rover station.....	48
Figure 3.2: An overview of the data recording times.....	50
Figure 3.3: Manfrotto tilted 15 degrees to West.....	54
Figure 3.4: KSAT Svalbard Satellite Station at Svalbard.....	58
Figure 3.5: Location of NYA1 reference station and base and rover stations.....	60
Figure 3.6: Location of base station and rover station at SVALSAT.....	61
Figure 3.7: Photo of rover station and base station at Svalbard.....	62
Figure 4.1: Scatter plot of DD Kinematic - true position of base station.....	65
Figure 4.2: Scatter plot of DD Kinematic - true position of rover station.....	66
Figure 4.3: GPS Single plan scatter plot.....	68
Figure 4.4: GPS Single height plot.....	68
Figure 4.5: Plot of the GPS Single pseudo-range residuals in times.....	69
Figure 4.6: GLONASS plan scatter plot.....	70
Figure 4.7: GLONASS plan position plot in time series.....	70
Figure 4.8: GLONASS height plot.....	71
Figure 4.9: GPS Dual plan scatter plot.....	72
Figure 4.10: GPS+GLONASS plan scatter plot .....	73
Figure 4.11: GPS+GLONASS height plot.....	74



Figure 4.12: Map of all IALA DGPS Reference Stations.....	75
Figure 4.13: Plots of SNR of GPS L1 and GPS L2.....	76
Figure 4.14: Plots of SNR of GPS L1, GPS L2, GLONASS L1 and GLONASS L2.....	77
Figure 4.15: Skyplots of GPS satellites and GLONASS satellites.....	79
Figure 4.16: Skyplot of the combined GPS+GLONASS satellites.....	80
Figure 4.17: The number of satellites by GPS and GLONASS.....	83
Figure 4.18: The number of satellites by GPS+GLONASS.....	84
Figure 4.19: A plot of GPS DOP values and number of satellites.....	85
Figure 4.20: A plot of GPS+GLONASS DOP values and number of satellites.....	86
Figure 4.21: Plots of multipath from tilt cycle 2B.....	89
Figure 4.22: Skyplot of GPS satellite G29 and GLONASS satellite R18.....	91
Figure 4.23: Plot of SNR, multipath and elevation of G29 R18.....	92
Figure 4.24: Skyplot of the antenna view.....	94
Figure 4.25: Plot of GLONASS number of satellites.....	95
Figure 4.26: Plots of GLONASS position in E-W, N-S and U-D.....	95
Figure 2.27: The plot of GPS+GLONASS satellites.....	97
Figure 4.28: Plot of the Rate of TEC Index at ground in Norwegian territory.....	99
Figure 4.29: Plot of the mean ROTI (TECU/min) in Norwegian territory.....	100
Figure 6.1: Polar bear at Svalbard.....	103

## **LIST OF TABLES AND DIAGRAMS**

Table 2.1: Table of GPS and GLONASS comparison.....	28
Table 4.1: The table is the accuracy and precision as performed by the GNSS.....	67
Table 4.2: Table of DOP average values of the long period.....	81
Table 4.3: The table is the accuracy and precision in the short period.....	82
Table 4.4: The table of GPS Single.....	93
Table 4.5: The table of GLONASS.....	94
Table 4.6: The table of GPS Dual .....	96
Table 4.7 The table of GPS+GLONASS.....	96
Table 4.8 The table of DGPS.....	98
Table 4.9 A table of the sun activity which occurred on 22 June.....	100
Diagram 3.1: Diagram of step 1 to 4 of the DD Kinematic approach.....	59
Diagram 3.2: Diagram of step 5 and 6 of the DD Kinematic approach.....	60

## **LIST OF ABBREVIATIONS**

AIS	Automatic Identification System
BDT	BeiDou Time
BPSK	Binary Phase Shift Keying
C/A	Coarse Acquisition
DBHZ	DeciBel Hertz
CDMA	Code Division Multiple Access
DD	Double Difference
DGPS	Differential Global Positioning System
DME	Distance Measuring Equipment
DoD	Department of Defence
DOP	Dilution Of Precision
DS-SS	Direct Sequence Spread Spectrum
ECDIS	Electronic Chart Display and Information System
EGNOS	European Geostationary Navigation Overlay Service
FDMA	Frequency Diversion Multiple Access
GDOP	Geometric Dilution Of Precision
GLONASS	GLobalnaya NAVigatsionnaya Sputnikovaya Sistema
GNSS	Global Navigation Satellite System
GPS	Global Positioning System
GPST	GPS Time
GSA	European GNSS Agency
HDOP	Horizontal Dilution Of Precision
HMI	Hazardously Misleading Information
IAC	Information Analytical Centre
IALA	International Association of Lighthouse Authorities
IGS	International GNSS Service

IMO	International Maritime Organization
ITR	International Terrestrial Reference System
ITU	International Telecommunication Union
KSAT	Kongsberg Satellite Services
LHC	Left Hand Circular Polarized
L1OF	L1 Open Frequency Diversion Multiple Access
NEP	North East Passage
NSR	North Sea Route
NYA1	Ny-Ålesund Reference Station 1
Ofcom	Office of Communications
PPD	Personal Privacy Device
PPP	Precise Point Positioning
PPS	Precise Positioning Service
PRN	Pseudo-Random Noise
PZ-90	Parametry Zemli 1990 (Earth Parameters 1990)
RHC	Right Hand Circular Polarized
RF	Radio Frequency
RINEX	Receiver INdependent EXchange format
RTK	Real-Time Kinematic
SBAS	Satellite Based Augmentation System
SNR	Signal to Noise Ratio
SPC	Satellite Prime Contractor
SPS	Standard Position Service
SDV	Standard DeViation
SVALSAT	KSAT Svalbard Satellite Station
TACAN	Tactical Air Navigation System
TEC	Total Electron Content
TDOP	Time Dilution Of Precision

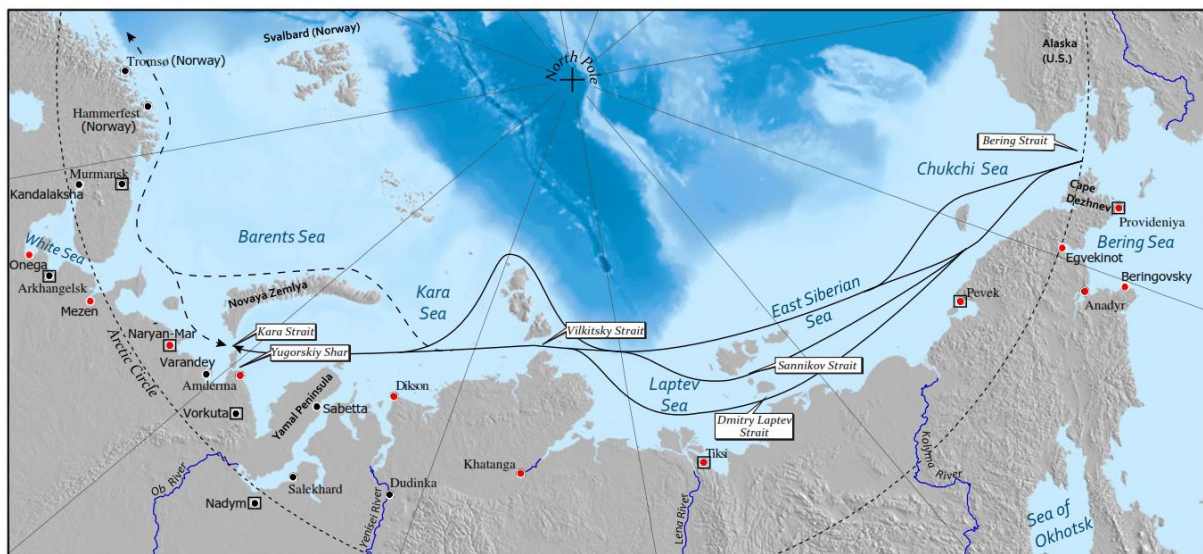
UTC	Universal Coordinated Time
USERE	User Equivalent Range Error
VDOP	Vertical Dilution Of Precision
WGS 84	World Geodetic System 84
WRC	World Radio-communication Conference

# 1 INTRODUCTION

## 1.1 Background

The Arctic sea ice extent is declining. Statistics from National Snow and Ice Data Centre 2015 states that the monthly June ice extent for 1979 to 2015 has declined 3.6% per decade relative to the 1981 to 2010 average. Climate Scientists simulations of future climate predicts the Arctic Ocean to be ice-free around summer 2052 (Sumner 2015).

In 2009 the German company Beluga Shipping sent one of its vessels on a journey along the Northeast Passage (NEP) to great fanfare. The cargo ship's journey was seen as the unofficial inauguration of the critical passage along the coast of Norway and Russia (Braw 2015). The transit statistics of civil vessels in NEP are as follows: 41 vessels in 2011, 46 in 2012, 71 in 2013 and 53 vessels in 2014 (Northern Sea Route Information Office 2015).



**Figure 1.1** Map of the Norwegian and Russian Arctic coasts, showing the NEP sea lanes. The solid line part is called Northern Sea Route by Russia. Settlements in red have port facilities. The squares are planned Search And Rescue stations (adopted from Buixadè 2015)

The sailing distance between Rotterdam in Europe and Yokohama in Asia via NEP is about 7010 nautical miles (depending of which shipping lane the ship uses in NEP) and is about 37% shorter than the sailing distance via Suez Canal (Buixadè 2015). The season for transit in NEP is limited to summer time when there is younger and thinner ice, free floating ice and ice-free conditions along the Western part and along the coastal areas. The harsh weather conditions, fog, low predictability of ice conditions and the remoteness and limited search and rescue capabilities increase the risk to operations in NEP and Svalbard area. Accidents happen and ship captains have experienced the slogan "Being at sea is risky, being at sea in ice is twice as risky, and being at sea in a convoy with an icebreaker present is three times the risk" (Østreng 2015).

The Government of Norway is responsible for the Norwegian part of NEP and Svalbard area. It is very concerned about the safety of personnel and material in this area using the Royal Norwegian Navy, the Norwegian Air Force and rescue helicopters as major players in surveillance and in search and rescue. The government encourages and supports research in the arctic area. This research in navigational technology in the arctic area is sponsored by The Competence Centre in Navigation, The Royal Norwegian Navy.

GPS is the most used GNSS system (Global Navigation Satellite System) in positioning and navigation in open waters and coastal waters on board civilian vessels using civil GPS signal L1 only. Since 2011 there have been two fully operational GNSS systems. New civil GNSS signal GPS L2C will be operational about 2017. GPS L5 will be operational about 2020 and GPS L1C about 2024. GLONASS L2OF (O=Open, F=FMDS) is already operational and GLONASS L3OC (C=CDMA) was available from 2013. New GNSS equipment is needed to exploit both systems combined and their new GNSS signals (Moore 2015).

According to (GSA 2015) the maritime GNSS components offered by manufacturers in March 2015 around 75% of the devices have implemented at least two GNSS

constellations. The most popular system after GPS is GLONASS. The largest maritime components manufactures offering multi GNSS equipment are FURUNO, TRIMBLE, NOVATEL, RAKON, OROLIA, SAMYUNG ENC, LAIRD and more.

The Arctic shipping routes compared to other shipping routes further South are affected by the fact that its Northern Latitude is higher than GNSS satellite's inclination angle relative to the equator and ionospheric irregularities due to aurora borealis (Bingley 2014).

## **1.2 Aims And Objectives Of The Research**

### **1.2.1 Hypothesis**

The investigation is based on the hypotheses:

- "The GNSS combination which the user GNSS equipment uses to determining position affects the accuracy and precision of the position as well the availability to GNSS satellites."
- "High number of satellites is assessed to offer higher precision and accuracy as well as increased redundancy."
- "GLONASS satellites are assessed to gain higher altitude than GPS due to higher satellites inclination angle to the Equator. This results in higher signal-to-Noise-Ratio (SNR) and better availability of the signals during ship movements (Roll and Pitch) or if close to Arctic mountains."
- "Dual frequency receivers increase the position accuracy compared to single frequency receivers due to the possibility to correct ionosphere biases."
- "Differential corrections are assessed to be received in some NEP area."
- "Combined GNSS receiver is assessed to gain high position accuracy and precision as well as higher number of satellites and increased redundancy."



### **1.2.2 Aim of the Research**

The aim of the research is to test the above hypothesis in the arctic area by comparing the effect of different GNSS combinations on the positioning accuracy and precision, availability of GNSS satellites, their SNR and redundancy.

### **1.2.3 Objectives of the Research**

In line with the defined aim of the research, the main objectives of the thesis are defined as:

- To learn and become familiar with the measuring equipment and processing tool and conduct test measurements and data collecting as well as processing the test data at the University.
- To conduct the preparation, records the data and collecting the GNSS raw data at Svalbard.
- To process the collected raw data at the University
- To conduct the analysis and compare the processed data
- To compare the results with results obtained by others' research

The research question is therefore:

- Which GNSS combination is advantageous in accurate and robust maritime navigation in the arctic areas around Svalbard and in the Northeast Passage for civilian vessels?

### **1.2.4 Thesis Outline**

Chapter 1 introduces of the arctic area and NEP and gives the later development of the shipping route and the background of the research. Development of GNSS satellite signals and GNSS equipment, offered by the maritime GNSS components manufactures, are also given. The aim and objectives of the research are presented.

Chapter 2 is the literature review and gives a brief overview of the GNSS systems and a look at the signal structure of GPS and GLONASS. Further, a comparison of GPS and

GLONASS is conducted and the GNSS system biases and errors are described. It also looks into the satellite constellation geometry and the vulnerability of GNSS systems. Finally, a description of RTKLIB, the data analysis software tool, used in the research is presented.

Chapter 3 describes the methods used in this research. The methodology of the three parts static measurements, ship moving simulation and sun activity are enlightened. The equipment used, test measurement, GNSS combinations and data recording are covered. The chapter describes also the data analysis techniques, how the location of the measurements was decided as well as the methodology of establishing true position of rover and base station. How the results of the following chapter are presented will be described and research design issues and limitations will be discussed.

Chapter 4 consist of the result and the discussion part. The result of the true position of rover and base station is defined. The GNSS combinations and the GPS and GLONASS systems are analysed in the long and short period. The accuracy and precision, SNR, skyplot and redundancy are discussed. The ship movement simulator is discussed with focus on multipath and accuracy. Finally the sun activity on 22 June will be discussed.

Chapter 5 presents a conclusion of the static periods and, ship moving simulation and the sun activity analysis.

Chapter 6 gives recommendations for further work.

## **2 LITERATURE REVIEW**

The late changes in the literature review are expanded regarding the comparison of GPS and GLONASS, as well as errors and bias affecting the accuracy and GNSS vulnerability. The red thread has been improved in accordance with the research aim and objectives in order to use the literature review as background and reference of the findings in the result and discussion chapters. General knowledge of GNSS, old information and previous conducted jamming trial has been removed.

### **2.1 Global Navigational Satellite Systems (GNSS)**

Global Navigational Satellite systems (GNSS) are the term for satellite based navigation systems with global coverage. GPS and GLONASS are both a one-way ranging system from the satellites to the users. The principle is for the users to find its position by measuring the distance to at least 4 satellites. There are two fully operational GNSS systems today (Bingley 2014).

In 1995 the Global Positioning System (GPS) became the first fully operational system with 24 satellites. GPS is developed and operated by the USA. Originally intended for the military but is today certainly the most used maritime positioning system in the civilian world (Bingley 2014). According to the GPS.gov (GPS 2015) the performance level of GPS Standard Positioning Service (SPS) Performance Standard for the GPS signal in space will provide a "Worst case" pseudo-range accuracy of 7.8 meters at a 95% confidence level.

The "GLObalnaya NAVigatsionnaya Sputnikovaya Sistema (GLONASS)" was the second fully operational system in 2011. GLONASS is operated by the Russian Aerospace Defence Forces for the Russian Government.

Other GNSS systems are in various stages of development, but not fully operational. China is developing and expanding their regional BeiDou system into a global system. The European Union is developing the Galileo system (Elmas 2013).

The market share of maritime GNSS units is only about 1% of the total number of GNSS units. Mobile phone GNSS units have the largest market share. The number of maritime GNSS units are according to GSA (GSA 2015) expected to almost double in the next ten years. FURUNO, OROLIA, NOVATEL, TRIMBLE, RAKON, SAMYANG ENC are the largest manufacturers of maritime GNSS component (GSA 2015).

The good and stable performance of GPS and GLONASS operational from 2011 and the expectation of Galileo and BeiDou (BDS) to be operational have made the International Maritime Organisation (IMO) MSC 95 (Maritime Safety Committee) in June 2015 to approve a new draft standard of "Performance Standards for Multi System Shipborne Radio Navigation Receivers". The performance standards aim to address the combined use of current and future radio navigation system (IMO 2015).

## **2.2 The Signal Structure Of Global Positioning System (GPS)**

Each GPS satellite signal consists of three components:

### **2.2.1 GPS Carrier Wave – Component One**

Each GPS satellite continuously transmits two radiofrequencies in the L-band referred as Link 1 (L1) and Link 2 (L2). The L-band covers frequencies between 1 GHz and 2 GHz, and is a subset of the ultra-high frequency (UHF) band. L1 and L2 are the GPS carrier waves. For the civilian users the second civil signal L2C is transmitting on the GPS satellites GPSIIR/IIR-M. The centre frequencies of L1 and L2C are:

$$L1: f_{L_1} = 1575.42 \text{ MHz}, \quad L2C: f_{L_2} = 1227.60 \text{ MHz}$$

The L1 carrier wave has a wavelength of about 19 cm and the L2C a wavelength of about 24 cm (Groves 2013). A third civil signal L5 was available on GPSIIF satellites from

September 2009. The fourth civil signal L1C will be on the block GPS III satellites. It will take time before these new signals are fully operational. However L2C is close to become operational when the last 3 GPS IIA satellites are retired (Moore 2015).

$$L5: f_{L_5} = 1176.45 \text{ MHz}, \quad L1C: f_{L_1} = 1575.42 \text{ MHz}$$

### **2.2.2 Ranging Code – Component Two**

The U.S. Department of Defence (DoD) offers two kinds of services. One for peaceful civil use called Standard Positioning Service (SPS), and one for DoD - authorized users called Precise Positioning Service (PPS) (Bingley 2014). The focus in the research is the SPS.

Each GPS satellite transmits a unique binary ranging code called the Pseudo-Random Noise (PRN) code for civilian users called Coarse/Acquisitions (C/A) on L1, and for authorized users Precise (P(Y)) on both L1 and L2 (Groves 2013). Each C/A code has a unique sequence of 1023 bits (called chips), which is repeated each millisecond. The duration of each C/A-code is about  $1 \mu\text{s}$ . The chip width or wavelength is about 300m (Bingley 2014).

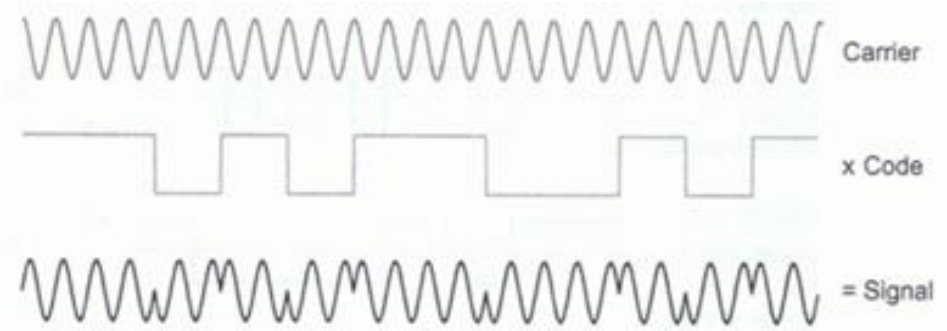
### **2.2.3 Navigation Data Message – Component Three**

Each satellite transmits a binary-coded message on L1 and L2 consisting of data of ephemeris (satellite health status and exact location data and velocity), clock bias parameters, and an almanac giving reduced-precision ephemeris data on all satellites in the constellation. The navigation message is transmitted at a leisurely 50 bits per second (bps) and a bits duration of 20 ms. The essential satellite ephemeris and clock parameters are repeated each thirty seconds (Leick et. al. 2015). Since April 2014 the civil navigation message has also been transmitted on L2C and L5 (GPS 2015).

### **2.2.4 Modulation - Ranging Code and Navigation Data**

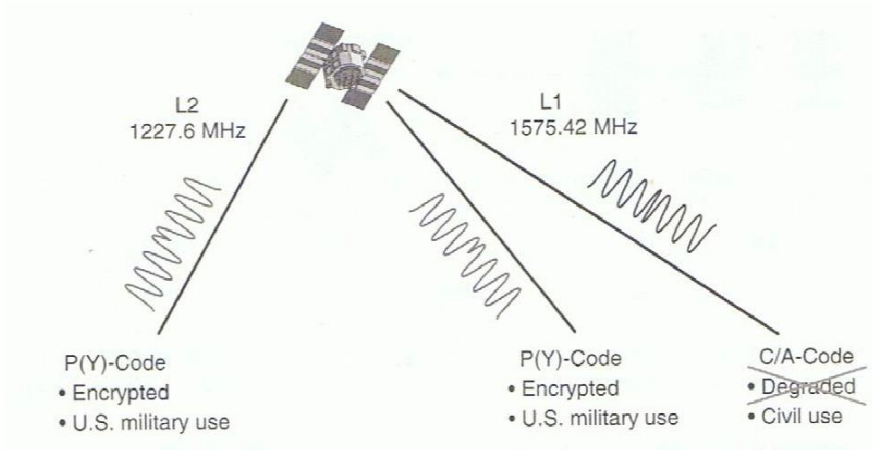
The binary ranging code is combined with the binary navigation data using modulo-2 addition: If the code chip and the data bit are the same (both are 0s or both are 1s), the result is 0; and if both are different, the result is 1. The composite binary signal is then impressed upon the carrier wave in a process called modulation. The specific form of

modulation used is called Binary Phase Shift Keying (BPSK): a 0 bit leaves the carrier signal unchanged; and a 1 bit multiplies the carrier by -1, which is equivalent to shifting the phase of the sinusoidal signal by 180°. At bit transitions from 0 to 1, or from 1 to 0, the phase of the carrier signal is shifted by 180° (Groves 2013).



**Figure 2.1** BPSK modulation of a carrier (not to scale) (Groves 2013)

Each GPS satellite generates two carrier wave signals on L1: - One generated by the clock (in-phase component) which is modulated by the ranging C/A-code. The other is obtained by shifting it in phase by 90° (quadrature component) which is modulated by the ranging P(Y)-code. The phase shift allowing a receiver to separate their modulating signals.



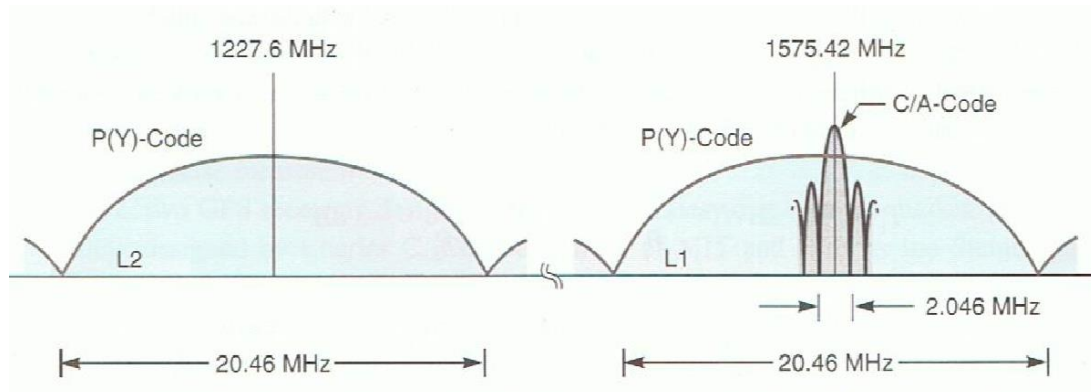
**Figure 2.2** Each GPS satellite transmitted three Binary Phase Shift Keying (BPSK) modulated signal two on L1 and one on L2 are shown (Misra & Enge 2006).

### 2.2.5 Code Diversion Multiple Access (CDMA)

The modulation transmission scheme is called Code Diversion Multiple Access (CDMA) which is a form of spread spectrum. This technique allows differentiating between the GPS satellites although they transmit on the same frequencies (Bingley 2014).

### 2.2.6 Direct Sequence Spread Spectrum (DS-SS)

The modulation of a carrier by a binary code spreads the signal energy, initially concentrated at a single frequency, over a wide frequency band: over 2MHz for the C/A-code and about 20 MHz for the P(Y)-code, centred at the carrier frequency. While the signal power is unchanged, this step reduces the power spectral density below that for the background RF radiation (Groves 2013).



**Figure 2.3** Power spectra of signals transmitted by a GPS satellite. The energy of the signal for civil users carrying a C/A-code on L1 is spread over a 2-MHZ-wide frequency band. The bandwidths of the signals for military users on L1 and L2 carrying a P(Y)-code are ten times wider (Misra & Enge 2006).

The primary reasons for using DS-SS in satellite navigation are:

Firstly the frequent phase inversions in the signal introduced by the PRN waveform enable precise ranging by the receiver.

Secondly, the use of different PRN sequences enables multiple satellites to transmit signals simultaneously and at the same frequency. A receiver can distinguish among these signals based on their different codes. For this reason, the transmission of multiple

DS-SS signals having different spreading sequences on a common carrier frequency is referred to as Code Division Multiple Access.

Third, the DS-SS provides significant rejection of narrowband interference (Kaplan & Hearty 2006).

### **2.2.7 Signal Power**

The GPS signals received on earth are very weak. The radio frequency (RF) power at the antenna input port of a satellite is about 50 watts, of which about half is allocated to the C/A-code, and the satellite antenna spread the RF signal evenly over the surface of the earth. The GPS signals are well below the background RF noise level sensed by the user antenna. The receiver uses the knowledge of the signal structure to extract the signal buried in noise and make precise measurements. If the noise level is raised by the interference the receiver may not be able to extract the signal. The low signal is the Achilles heel of GPS/GNSS which makes the systems vulnerable. The GPS minimum received signal power specifications states that the minimum received power level for the user on the earth should be -158.5 dBW for the C/A-code. The normalized minimum power for GLONASS should not be less than -157 dBW on G1 (Misra & Enge 2006).

The new signals on L2C and L5 have increased signal power (GPS 2014).

### **2.2.8 Signal to Noise Ratio**

(Inside GNSS 2014) in article Measuring GNSS Signal Strength describes carrier to noise density ratio as follows: GPS receivers built for various applications, such as handhelds, automobiles, mobile phones, and avionics, all have a method for indicating the signal strength of the different satellites they are tracking. Some receivers display the signal strength in carrier-to-noise density (C/N<sub>0</sub>) or signal-to-noise ratio (SNR). C/N<sub>0</sub> is usually expressed in decibel-Hertz (dB-Hz) and refers to the ratio of the carrier power and the noise power per unit bandwidth.



For the GPS L1 C/A signal, one can consider the received signal power as the power of the original unmodulated carrier power (at the point of reception in a receiver) that has been spread by the spreading (ranging) codes when transmitted from a satellite. We can express C/N0 as follows:

$$C/N_0 \text{ (dB-Hz)} = C - (N - BW) = C - N_0 = \text{SNR} + BW \quad (2.1)$$

Where:

C is the carrier power in dBm or dBW;

N is the noise power in dBm or dBW;

N0 is the noise power density in dBm-Hz or dBW-Hz;

BW is the bandwidth of observation, which is usually the noise equivalent bandwidth of the last filter stage in a receiver's RF front-end.

Typical values in an L1 C/A code receiver are as follows:

C/N0: ~ 37 to 45dB-Hz

(Bingley 2014) informs that C/No is mainly varying with the elevation of the arriving signal, as the signal from high elevation satellites has higher signal strength and is less affected by noise as it reaches the receiver.


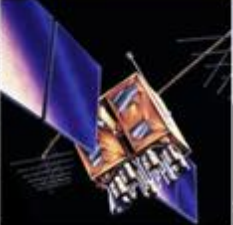
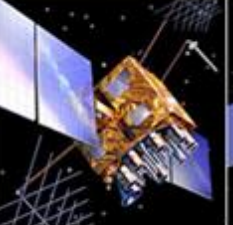
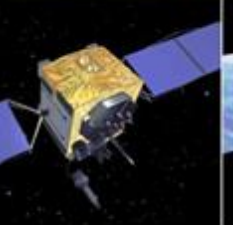

The RTKLIB use SNR (dBHz).

### **2.2.9 Operational GPS Satellites – Status at 9 August 2015**

GPS satellite type Block IIA and Block IIR transmit carrier wave L1 and L2. They transmit the modulated ranging C/A code on L1, and the ranging P(Y) code on both L1 and L2.

Block IIR-M transmits on L1 and L2, and the same ranging codes as Block IIA and Block IIR. In addition the BLOCK IIR-M now transmits the second civil ranging code L2C (C for civil) on L2. There are 17 satellites which transmit the L2C signal.

The satellite Block IIF transmits the same signals as Block IIR-M, but has started to transmit also on Link 5 (L5) in addition to L1 and L2 (Space segment 2015). There are 10 satellites which transmit the L5 signal.

LEGACY SATELLITES		MODERNIZED SATELLITES		
				
BLOCK IIA	BLOCK IIR	BLOCK IIR(M)	BLOCK IIF	GPS III
<b>3</b> operational	<b>12</b> operational	<b>7</b> operational	<b>9</b> operational	In production
<ul style="list-style-type: none"> <li>Coarse Acquisition (C/A) code on L1 frequency for civil users</li> <li>Precise P(Y) code on L1 &amp; L2 frequencies for military users</li> <li>7.5-year design lifespan</li> <li>Launched in 1990-1997</li> </ul>	<ul style="list-style-type: none"> <li>C/A code on L1</li> <li>P(Y) code on L1 &amp; L2</li> <li>On-board clock monitoring</li> <li>7.5-year design lifespan</li> <li>Launched in 1997-2004</li> </ul> <a href="#">VIEW AIR FORCE FACT SHEET →</a>	<ul style="list-style-type: none"> <li>All legacy signals</li> <li>2nd civil signal on L2 (L2C) <a href="#">LEARN MORE →</a></li> <li>New military M code signals for enhanced jam resistance</li> <li>Flexible power levels for military signals</li> <li>7.5-year design lifespan</li> <li>Launched in 2005-2009</li> </ul> <a href="#">VIEW AIR FORCE FACT SHEET →</a>	<ul style="list-style-type: none"> <li>All Block IIR(M) signals</li> <li>3rd civil signal on L5 frequency (L5) <a href="#">LEARN MORE →</a></li> <li>Advanced atomic clocks</li> <li>Improved accuracy, signal strength, and quality</li> <li>12-year design lifespan</li> <li>Launched since 2010</li> </ul> <a href="#">VIEW AIR FORCE FACT SHEET →</a>	<ul style="list-style-type: none"> <li>All Block IIF signals</li> <li>4th civil signal on L1 (L1C) <a href="#">LEARN MORE →</a></li> <li>Enhanced signal reliability, accuracy, and integrity</li> <li>No Selective Availability <a href="#">LEARN MORE →</a></li> <li>Satellites 11+: laser reflectors; search &amp; rescue payload</li> <li>15-year design lifespan</li> <li>Begins launching in 2016</li> </ul> <a href="#">VIEW AIR FORCE FACT SHEET →</a>

**Figure 2.4** Type and status of GPS satellites at 9 August 2015 (Space segment 2015).

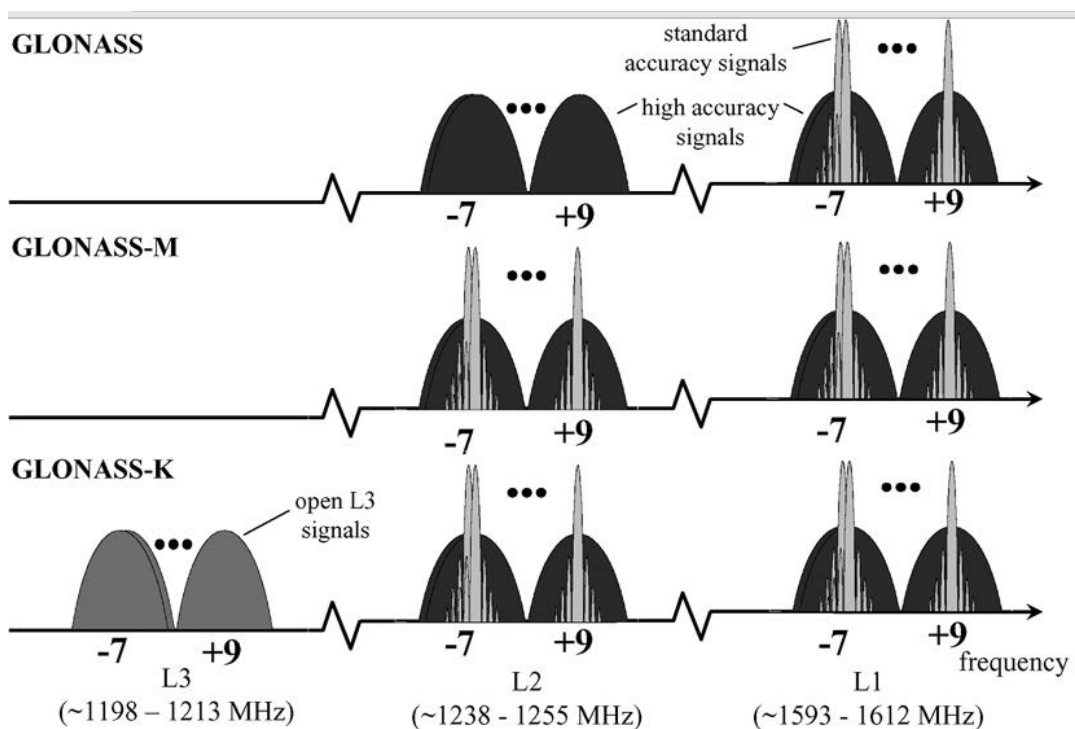
### 2.3 The Signal Structure Of GLONASS

GLONASS has much in common with GPS in terms of its system architecture, origin as a military system, and even the terminology: C/A-code, P-code, Standard Positioning

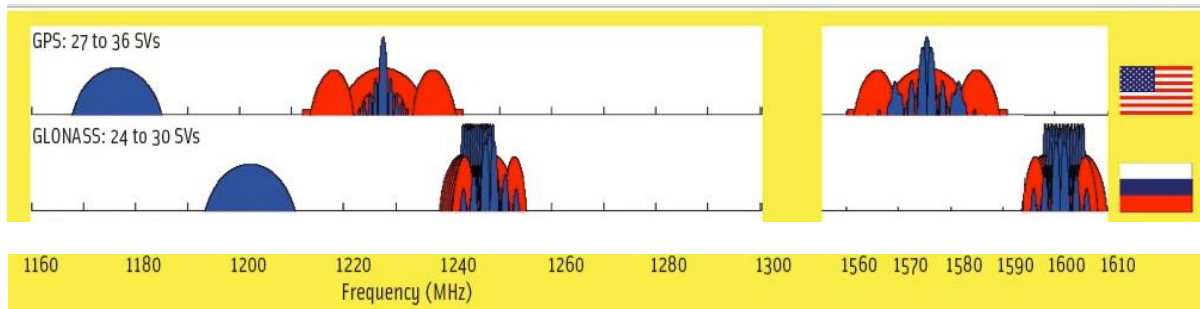
Service (SPS) and Precise Positioning Service (PPS). GLONASS also have L1 and L2 as carrier waves.

### 2.3.1 GLONASS Satellite Signals

Like GPS, each satellite transmits three signals: On carrier wave L1, a C/A-like, 511-chip long PRN code repeated with a period of 1 ms; and on both L1 and L2, a 511k-chip long PRN code with a period of 1 s. The chipping rate of the GLONASS SPS and PPS signals is half those of GPS. But the navigation data message is transmitted at the same rate as GPS-50bps (Groves 2013).



**Figure 2.5** Power spectra of signals transmitted by GLONASS satellites. The high accuracy code is transmitted on both L1 and L2, and the Standard accuracy code on L1 (all satellites) and L2 (GLONASS-M satellites) (IEEE Explore 2014).



**Figure 2.6** Power spectra of signals of both GPS (top) and GLONASS (inside GNSS 2014)

### 2.3.2 Frequency Diversion Multiple Access (FDMA)

Unlike GPS, which uses CDMA signalling scheme, GLONASS employs Frequency Diversion Multiple Access (FDMA) scheme (Elmas 2013): The same PRN is transmitted by each satellite, but at different RF carrier frequencies using a 14 channel FDMA. The RF carriers are channelized, and at L1 the channel spacing is 0.5625 MHz with 7 channels lower than the centre frequency, 1 channel at the centre frequency of 1602 MHz and 6 channels higher. The lowest channel has thus centre on 1598.06 MHz and the uppermost channel has centre on 1605.38 MHz. The 24 satellites get by with 14 channels by assigning the same channel to satellites on the opposite side of the earth. Difference in the carrier frequencies leads to low cross correlations between the FDMA signals (Groves 2013).

### 2.3.3 Operational GLONASS Satellites – Status at 9 August 2015

23 operational GLONASS Satellite type M transmit carrier wave on L1OF and L2OF.

1 GLONASS M satellite is in maintenance.

2 GLONASS M satellites are under check by the Satellite Prime Contractor (SPC) and two M satellites are in flight tests phase.

2 GLONASS K1 satellites which transmit on the same frequencies as the M satellites also transmit on L3OC does flight testing (GLONASS IAC 2015).

## 2.4 GLONASS And GPS Comparison

<b>GLONASS</b>	<b>Parameter</b>	<b>GPS</b>
<b>24</b>	<b>Number of Satellites</b>	<b>24</b>
<b>3</b>	<b>Orbital Planes</b>	<b>6</b>
<b>64.8°</b>	<b>Inclination</b>	<b>55°</b>
<b>19,100 km</b>	<b>Orbit Altitude</b>	<b>20,233 km</b>
<b>1597-1617 MHz 1240-1260 MHz FDMA</b>	<b>RF Frequency</b>	<b>L1:1575 MHz L2: 1227 MHz CDMA</b>
<b>8 day ground repeat</b>	<b>Ground Tracks</b>	<b>Ground repeat 4 mins earlier each day</b>
<b>511 kbits/sec</b>	<b>C/A Code</b>	<b>1023 kbits/sec</b>
<b>5.11 MHz</b>	<b>P Code</b>	<b>10.23 MHz</b>
<b>P,V,T</b>	<b>Ephemeris</b>	<b>Keplerian</b>
<b>Keplerian</b>	<b>Almanac</b>	<b>Keplerian</b>

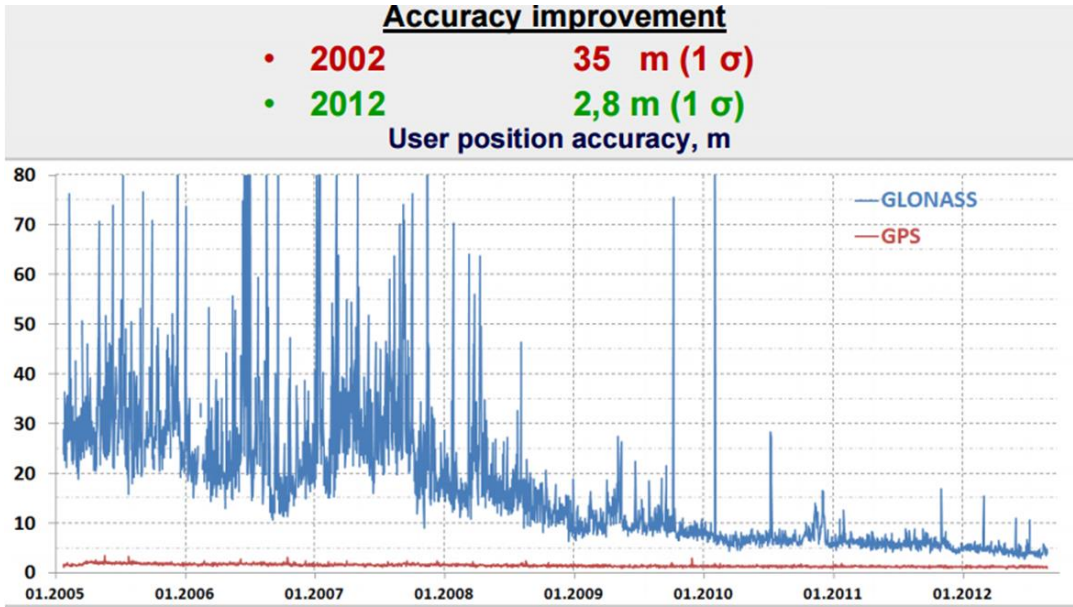
**Table 2.1** Table of GPS and GLONASS comparison (Moore, NGI, University of Nottingham)

The 24 operational GLONASS satellites orbits in 3 orbital planes with 8 satellites in each plane while GPS have the same number of satellites in 6 orbital planes and 4 GPS satellites in each planes. The satellites planes of GLONASS has an inclination angle of 64.8° almost 10° higher than GPS and thereby gets higher elevation in the Arctic. The orbital altitude of GLONASS is closer to Earth at 19.100km altitude compared to GPS satellites altitude at 20.233km. This means that the GLONASS satellites travel faster than the GPS satellites. The ground tracks of GLONASS are repeated every 8 day but the ground tracks of GPS are repeated 4 minutes earlier each day (23hours 56minutes) (Moore 2015).

The receiver approach to identification of satellites is also different. GPS uses timing code (CDMA) to identify satellites while GLONASS satellites are identified by the frequency (FDMA). The carrier frequencies of GLONASS are spread over a larger wide frequency band than GPS and were registered as more robust under the jamming trials conducted by Glomsvoll (Glomsvoll 2014). It is interesting to note that GLONASS on the GLONASS

K1 satellites has started using CDMA signals on L3. GLONASS K2 satellites will have CDMA on L1, L2 and L3 signals in addition to the FDMA signals on L1 and L2 (Moore 2015). The reason for adding the CDMA is the compatibility of GLONASS with GPS and other future GNSS systems. The carrier phase approach solution is different. GPS carrier phase use integer number of ambiguity and can gain fix solution, but the carrier phase on GLONASS does not use integer but real numbers gaining only float solution as a result. The chipping rate of C/A code is different as GPS has 1023 kbits/sec and GLONASS has about half (511 kbits/sec) giving GLONASS the potential of better ranging and shorter theoretical multipath error (Moore 2015).

The quality of the satellite clocks is different as GPS satellites have state of the art quality atomic clocks. The GLONASS satellite clocks traditionally have been much cheaper and of worse quality with lower accuracy as a result. The GLONASS modernization program gain to improve the clock stability using filters on M satellites and improved satellite clock quality in the K satellites (NAVIPEDIA 2015).



**Figure 2.7** The accuracy of GLONASS compared to GPS (GLONASS IAC 2015)

There has been a major difference in accuracy between GPS and GLONASS during the last 10 years. The GPS accuracy is stable and far better than GLONASS. However, as we see in figure 2.7 since the GLONASS was fully operational in 2011 the GLONASS accuracy has been improved. The research accuracy results are assessed to demonstrate a similar pattern between GPS and GLONASS.

The coordinates used by the two systems are also different. GPS uses World Geodetic System 84 (WGS 84) which uses location of the North Pole in 1984 as reference. GLONASS uses a coordinate datum Parametry Zemli 1990 (PZ-90) (Earth Parameters 1990) which uses location of the North Pole as an average of its position from 1990 to 1995. However, the GLONASS coordinate system version PZ-90.11 was tied to the International Terrestrial Reference System (ITR) at epoch 2011.0 at centimeter level in 31 December 2013. The aim of changing to PZ-90.11 was to improve the interoperability with other GNSS systems.

The approach of time is also different. GPS Time (GPST) = Universal Coordinated Time (UTC) + 17 seconds (included the leap second 30 June 2015). When a leap second happened the change was easily applied to the GPST. However, when a leap second happen the GLONASS time scale implements leapt seconds like UTC and this has caused problem (MOORE 2015).

Time is the key to combine two and more GNSS systems and all GNSS systems use UTC as reference. The time status after the last leap second is (Moore 2015)

- GPS Time = UTC + 17 seconds (2.2)

- GLONASS Time = UTC + 3 hours -  $\tau$  where  $|\tau| < 1$  milisec. (2.3)

- Galileo System Time (GST) = UTC+4 seconds (2.4)

- BeiDou Time (BDT) = UTC + 3 seconds (2.5)

The ephemeris parameter is also different as GPS broadcast Keplerian ephemeris parameters but the GLONASS broadcasts raw Cartesian ephemeris parameter which consists of the satellite position, satellite velocity, and time (Moore 2015).

The control segment of GPS and GLONASS are also different as the GPS has its ground stations around the globe that monitor the signals transmitted by the GPS satellites 24 hours a day. The control segment of GLONASS has been mostly inside the territory of Russia. However both systems are running modernization programs of their control segments. GPS is introducing modern technologies throughout space and control segments and legacy computers and communications systems are being replaced with a network-centric architecture which allows more frequent and precise satellite commands that will improve accuracy for everyone (GPS 2015). GLONASS adds more reference stations and six of them outside the Russian territory among them Bellingshausen and Novolazarevskaya bases in Antarctica (NAVIPEDIA 2015).

There is a huge difference in the user segment when it comes to the number of users of the two systems. The GPS system is by far the most used system including also the maritime stand-alone pseudo range GNSS equipment (Bingley 2014). This will change because according to GSA (GSA 2015) around 75% of all maritime GNSS devices offered by the manufacturers in March 2015 have implemented at least two constellations. The most popular GNSS system after GPS is GLONASS.

In his Ph.D. dissertation *The Performance of Hybrid GPS and GLONASS* Baker concluded with the main area of differences which create challenges in the interoperability of GPS and GLONASS to be the coordinate reference system and the time reference system (Baker, 2001). In 2015 the GLONASS has adjusted their coordinate system and time reference system making it interoperable with other GNSS systems. Manufactures offers maritime GNSS equipment also including GLONASS.



## **2.5 GNSS System Biases And Errors**

Bias is caused by a physical phenomenon as ionosphere and troposphere and error are quantities remaining after a bias have been mitigated to some extent (Bingley 2015).

### **2.5.1 Satellite Ephemeris Errors**

Over time the satellites accumulate some minor errors in their orbits. The satellites send broadcast ephemeris or mathematic predicted ephemeris as updated orbital information on top of the code signals but still there are some errors between the actual satellite position and the position expected by the receiver. "*The satellites are not where they say they are*" (Moore 2015). The errors can be mitigated by using predicted precise ephemeris from service providers such as as Satellite-Based Augmentation Systems (SBAS) (Moore 2015). Europe has the European Geostationary Navigation Overlay Service (EGNOS). However, the geostationary EGNOS satellite does not cover the arctic area around Svalbard and latitudes above 70°N in the NEP (EGNOS 2015). The errors in GPS broadcast ephemeris were 2m in 2001, improved to 1.6m in 2004 and 1m in 2010 (Bingley 2014).

Broadcast ephemeris was used in the research.

### **2.5.2 Satellite Clock Error**

The satellites clocks are highly accurate but they still accumulate some errors over time. This is calculated daily by the ground control stations and transmitted to the satellites to update the satellite broadcast ephemeris. As a system based on time errors in satellite clock offset propagate directly to errors in receiver coordinates. In the civil vessels stand-alone positioning a clock error of 5ns of each satellite in the broadcast ephemeris propagates to a 1.5m plan position error (Bingley 2014).

### **2.5.3 Ionospheric Bias**

High energy radiation (mostly in the form of UV and X-ray) and emissions from the surface of the sun influence Earth's upper atmosphere causing heating in the region. The atmospheric layer of altitude from about 100 to 1000 km is known as the ionosphere,

where solar radiation strips off electrons from atoms leading to an ionized gaseous medium, known as plasma. In addition to electrons being stripped off, a recombination process (by which a free electron is captured by a positive ion) also takes place. Low "atomic" density due to low gravitational force at these aforementioned altitudes leads to a low rate of recombination letting free ions and electrons dominate the ionosphere. It is measured in Total Electron Content (TEC) which is the total number of electrons integrated between two points along a tube of one meter squared cross section (Elmas 2013).

The TEC is driven by the sun's activity and its known periodicities as an 11 year's sunspot cycle, seasonal cycle and diurnal cycle. The magnetic storms can give a sizeable irregular pattern. GNSS signals are in the microwave part of the electromagnetic spectrum in order to reduce the effect of ionosphere and have less effect at higher frequencies. The ionospheric delay of satellite signals causing the pseudo-ranges to be too long is a function of TEC, carrier frequency and elevation angle. The largest bias in stand-alone positioning in plan is caused by the ionosphere. In stand-alone positioning with simple models there may still be a 10m plan position error (Moore 2015).

The secondary effect is the attenuation of the signal strength (Moore 2015).

The ionospheric scintillation activity which causes short-time fluctuations in received signal phase and amplitude depends on solar and geomagnetic activity, season, local time and the location. It is largest at the poles and equatorial regions (Moore 2015).

Mitigation strategies are to use dual frequency receivers to measure two or more frequencies to calculate ionospheric free pseudo-range and remove about 98% of the ionospheric effect. Single receivers can use the broadcast parameters in the navigation message which includes values of the parameters of a simple ionospheric model to mitigate the ionospheric bias and remove about 50% of the bias (Moore 2015).

The research used broadcast parameters as ionospheric corrections.

#### **2.5.4 Tropospheric Bias**

The tropospheric bias slows the signals, bending it due to refractions. There are two kinds of tropospheric bias delays: the hydrostatic component (dry component) and the wet component. The hydrostatic component is a function of atmospheric pressure, temperature and elevation angle and covers about 80 to 90% of the tropospheric bias. The wet component of partial water vapour and elevation angle constitutes about 10 – 20% of the tropospheric bias. The bias depends strongly on the elevation angle (Moore 2015).

Mitigation strategies are to compute dry air effect such as atmospheric pressure and temperature measurements. This has approx. 90% effect. Blind models based on latitude, altitude and day of year are also being used. The second largest bias in stand-alone positioning in plan is caused by the troposphere bias. In stand-alone positioning with simple models there may be a 2m plan position error (Moore 2015).

The Saastamoinen tropospheric model which assumes that the dry atmosphere is in hydrostatic equilibrium was used in the research.

#### **2.5.5 Multipath**

Multipath occurs when a satellite signal arrives at the receiver antenna by more than one path. Multipath signals are delayed through reflection from surfaces local to the satellite antenna relative to the true signal, and have a lower signal to noise ratio. Vessels on high seas will gain multipath reflected by the sea (large reflection area), superstructure and masts close to GNSS antenna. The ships roll and pitch movements and changes in course will change the local environment of multipath (Bingley 2014).

The size of error in stand-alone positioning is signal chip wavelength dependent. The maximum theoretical multipath error in a code observable is one chip length or about 290m for GPS L1 C/A code and about 145m for GLONASS L1. In practice 2 – 20 meters is

typical. Signals from low elevation satellites will be particularly susceptible to multipath effects (Moore 2015).

Mitigation strategies are to use high chipping rate signals (GLONASS chipping rate in combined GPS/GLONASS receivers). The internal receiver techniques narrow correlators or multi antenna site measurements may mitigate multipath. Low multipath antennas may have choke ring antenna or good axial ratio antenna. GNSS signals are Right Hand Circular Polarized (RHC). If the signals hits and reflects from the sea, it becomes Left Hand Circular Polarized (LHC). A good axial ratio antenna rejects LHC signals (Moore 2015).

### **2.5.6 Receiver Errors**

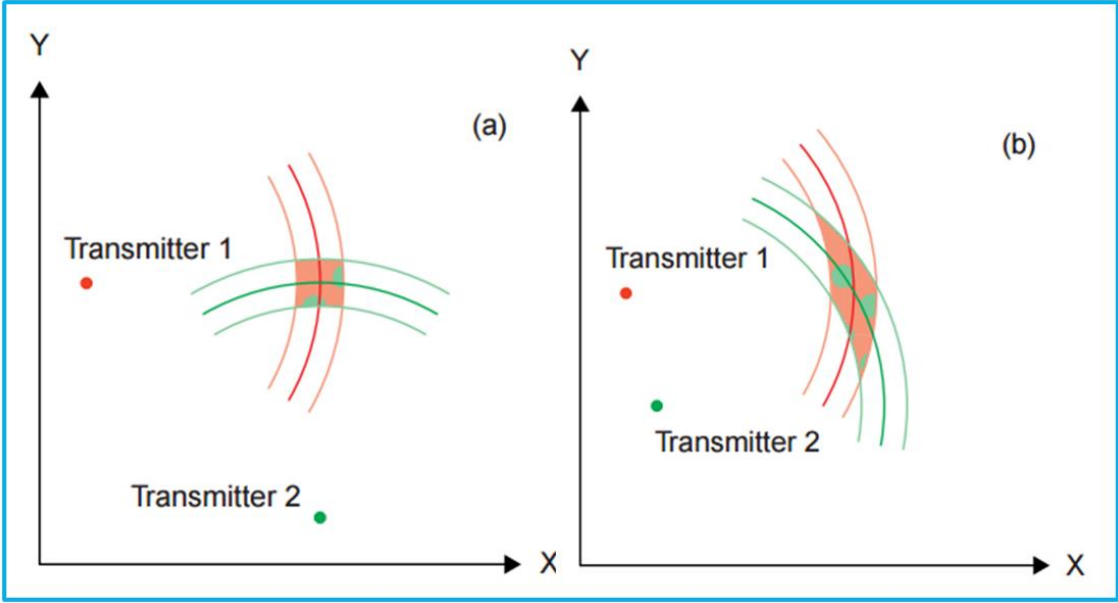
The receiver clock offset is being solved for in the stand-alone pseudo-range least square observation equation. Noise can affect the correlation peak causing tracking offsets. High background noise can camouflage the code signal. The receiver code noise is a white-like error which affects the code measurements. It can be smoothed using a low pass filter down to about 50 cm on L1 (NAVIPEDIA 2015). The size of receiver errors depends on the quality of user antenna and receiver (Moore 2015).

## **2.6 GNSS Satellite Constellation Geometry**

### **2.6.1 DOP**

A set of satellites which are more spread out in the sky will provide a more accurate position than a set of satellites that are close to each other. This concept is the Geometric Dilution of Precision (GDOP). Low DOP value represents a better positional precision caused by the wider angular separation between the satellites (Langley 1999).

It can be illustrated by a simple example where a receiver measures the range to two transmitters. The range from transmitter 1 to the receiver is illustrated with the bold red circular line and the thinner red lines show the uncertainties. A green line is used for transmitter 2. The receiver position is at the intersection of the green and red lines. Due to the uncertainties there is not a single intersection but a small area.



**Figure 2.8** Illustrating DOP - In (a), the transmitters are placed with wide angles relative to the observer. In (b), transmitter 2 is moved closer to transmitter 1 and increasing the DOP (Langley 1999).

To the left plot (a) the transmitters are 90° apart relative to the receiver. This results in a relatively small area of uncertainty. To the right plot (b) the transmitters are closer together in the X direction. This results in a larger uncertainty area for the receiver. The precision in plot (b) is diluted in comparison to plot (a) (Langley 1999).

The same concept is applicable for the positioning of a receiver in three dimensions using satellites with both positioning and timing errors. In general the DOP values get smaller when more satellites are used for a solution. It is possible to look at specific components

as horizontal coordinate (HDOP), vertical coordinate (VDOP) or the clock offset (TDOP).

They can be expressed as (Langley 1999)

$$\text{HDOP} = \frac{\sqrt{\sigma_E^2 + \sigma_N^2}}{\sigma} \quad (2.6)$$

$$\text{VDOP} = \frac{\sigma_U}{\sigma} \quad (2.7)$$

$$\text{TDOP} = \frac{\sigma_T}{\sigma} \quad (2.8)$$

They are related to the GDOP according to

$$\text{GDOP}^2 = \text{HDOP}^2 + \text{VDOP}^2 + \text{TDOP}^2 \quad (2.9)$$

Where:

$\sigma_E$ ,  $\sigma_N$  and  $\sigma_U$  are the *standard deviation* of the receiver position in the *East, North and Up* components.

$\sigma_T$  is the *standard deviation* of the receiver clock offset estimate.

$\sigma$  is the total *User Equivalent Range Error (UERE)*.

## 2.7 GNSS System Vulnerability

Failures in the GPS satellite and control system have occurred. 1 January 2004 a significant GPG anomaly “*affected precise timing and navigation users over large portions of Europe, Africa, Asia, Australia, and...North America... and resulted in the transmission of Hazardously Misleading Information (HMI)*”. It was a SVN23 clock failure (Moore 2015).

Failures caused by human factors such as human errors, over-reliance of GNSS, lack of knowledge of GNSS and lack of training are increasing the vulnerability of GNSS systems (Moore 2015).

### **2.7.1 Unintentional Interference**

Radio frequency signals from any undesired source that are received by a GNSS receiver are considered as interference. GNSS bands are protected by international agreements World Radio-communication Conference (WRC) held every third year in accordance with the constitution of International Telecommunication Union (ITU) (Moore 2015).

L1 band is generally only for GNSS. L2 was designated co-primary for radiolocation services. However, L2 does in some areas share the band with Air Traffic Control (ATC) radars and some types of military radars. L2 is also fixed to mobile communications service. L5 band of aeronautical radio-navigation is shared with the Distance Measuring Equipment (DME) ground transponder-based radio navigation and the DME component in Tactical Air Navigation System (TACAN) used by military aircraft (Moore 2015).

An example where transmissions in neighbouring frequency spill over into GNSS band is the LightSquared licenses to use L-band spectrum for mobile satellite service from SkyTerra. Despite the protection and separation of bands the power of LightSquared interfered with GNSS due to the need of extra wide bandwidth required for combined GPS+GLONASS receivers (Moore 2015).

Interference caused by faulty antennae, broken or corroded coaxial shielding of GNSS receivers can happen and affect nearby receivers up to 100m (Moore).

Natural causes generated from the sun can also give interference. Solar flares can disrupt GNSS equipment. Significant loss of redundancy in the number of tracked satellites can occur during a scintillation event. For instance, a solar radio bust can leave receivers unable to achieve a positioning solution due to tracking fewer than 4 satellites (Elmas 2013). The research will investigate the sun activity on 22 June using NYA1 Reference Station on Svalbard.

### **2.7.2 Intentional Interference**

Jamming is defined as "*the emission of sufficient Radio Frequency (RF) energy of sufficient power and with the proper characteristic to prevent receivers in the area from tracking the GPS signal*" (Volpe 2001:30).

There is a variety of available jammers on the market as Personal Privacy Device (PPD). The privacy concerns may be linked to an urge to prevent you from being tracked by your employer. Other motivations can be criminal activity or terrorism. In Europe, it is illegal to operate but not to own a jammer. More powerful jammers are also manufactured, but the most powerful jammers are for governmental use and have restrictions for sale and export (Moore 2015).

Spoofing is intentional "*transmission of false GNSS signals intended to cause the receiver to lock onto incorrect transmissions*" (Moore 2015). A simple spoof is enough to confuse the receiver. Todd Humphries, University of Texas, demonstrated spoofing on a yacht in June 2013 and "*fooled it to believe it was off-course, triggering course corrections which steered it off-course*" (Moore 2015).

Meaconing is rebroadcasting genuine signals and can act as a misleading beacon. It is not permitted to use by the Office of Communications (Ofcom) (Moore 2015).

In 2014 Glomsvoll conducted a dynamic jamming test north of the polar circle on board the Norwegian Coast Guard Vessel *Farm*. *Farm* sailed towards a jammer mounted on land causing the GNSS equipment to lose her positioning solution and give misleading information of course and speed on the Electronic Chart Display Information System (ECDIS) (Glomsvoll 2014).



## **2.8 GNSS Positioning Approaches**

### **2.8.1 Principle of Stand Alone Pseudo Range Positioning**

The principle of how GNSS systems work is simple and is based on time. GNSS relies on calculating the distance from the receiver to a satellite with a known position based on the time-in-flight of a radio signal sent from the satellite. Given the range measurements from three different satellites and their spatial locations the Cartesian position X, Y, Z can be calculated via triangulation. However, all satellites contain precise synchronized clocks. The receivers generally have a much less precise crystal oscillator clock which is not synced with the satellites. The distance measured to each satellite is therefore corrupted by the timing error between the satellite clocks and the clock in the receiver. The numbers of unknowns are therefore four: the Cartesian X, Y, Z and the time. To solve these four unknowns the receiver requires at least four satellites to compute the position of the receiver (Bingley 2014).

### **2.8.2 Stand Alone Pseudo Ranges**

User receiver measurements of pseudo-range observations:

The receiver receives incoming code signals using one channel per satellite unique code signal. It creates replica signals and uses code cross correlation of the incoming and replica signals to calculate the time-of-flight, -assuming the satellite and receiver clocks are synchronized. The difference in time between the transmitted code from satellite and the replica code generated in receiver multiplied by the speed of light is the Pseudo-range. Dr Bingley (Bingley 2014) defines measure of range using pseudo-range as: "*A pseudo-range is a direct measure of the one-way range (distance) from a satellite to a receiver, based on code (cross) correction of the incoming and replica signals to calculate the time-of-flight, and multiplying this by the speed of light*".

The pseudo-range observation equation for stand-alone is (Bingley 2014)

$$PR_r^S(\tau_r) = \rho_r^S(T^S, T_r) + c [ \delta\tau_r(\tau_r) - \delta t^S(t^S) ] + \text{dion}_r^S + \text{dtrop}_r^S + v_r^S \quad (2.10)$$

Where

$PR_r^S(\tau_r)$  is the *pseudo-range* between satellite  $s$  and receiver  $r$ ...  
in the *receiver time frame* of receiver  $r$ .

$\rho_r^S(T^S, T_r)$  is the *geometric range* between satellite  $s$  and receiver  $r$ ...  
in the *true GPS time frame*.

$c$  speed of light in vacuo.

$\delta\tau_r(\tau_r)$  is the *receiver clock offset* for receiver  $r$ ...  
in the *receiver time frame* of receiver  $r$ .

$\delta t^S(t^S)$  is the *satellite clock offset* for satellite  $s$ ...  
in the *satellite time frame* of satellite  $s$

$\text{dion}_r^S$  is the modelled bias due to ionospheric delay between satellite  $s$  and receiver  $r$ .

$\text{dtrop}_r^S$  is the modelled bias due to tropospheric delay between satellite  $s$  and receiver  $r$ .

$v_r^S$  is the observation residual.

The three-dimensional coordinates of satellite  $s$  and receiver  $r$  are in the *geometric range*,  
as...

$$\rho_r^s = \sqrt{[(X^s - X_r)^2 + (Y^s - Y_r)^2 + (Z^s - Z_r)^2]} \quad (2.11)$$

Where

$(X^s, Y^s, Z^s)$  are the Cartesian *coordinates* of satellite  $s$ ...

$(X_r, Y_r, Z_r)$  are the Cartesian *coordinates* of receiver  $r$ .

Least square implementation is used to solve the Cartesian coordinates of user receiver's four or more pseudo-range observation equations. Least square is a standard approach in regression analysis to the approximate solution where sets of equations where there are more equations than unknowns. "Least squares" means that the overall solution minimizes the sum of the squares of the errors made in the results of every single equation (Smith 2014).

The typical notation for the least squares observation equation is (Bingley 2014)

$$A \cdot x = b + v \quad (2.12)$$

Where

$A$  is a matrix containing the coefficients of the observation equation.

$x$  is a vector containing the corrections to the unknown parameters in the observation equation.

$b$  is a vector containing the *observed-computed* values.

$v$  is a vector containing the residuals.

Considering one receiver (a) and four satellites (e, n, o and v) a least square solution could be set up with the following A matrix and x, b and v vectors (Bingley 2014).

Where  $A \leq 1$

$$A = \begin{bmatrix} \frac{-(X^e - X_a)}{\rho_a^e} & \frac{-(Y^e - Y_a)}{\rho_a^e} & \frac{-(Z^e - Z_a)}{\rho_a^e} & 1 \\ \frac{-(X^n - X_a)}{\rho_a^n} & \frac{-(Y^n - Y_a)}{\rho_a^n} & \frac{-(Z^n - Z_a)}{\rho_a^n} & 1 \\ \frac{-(X^o - X_a)}{\rho_a^o} & \frac{-(Y^o - Y_a)}{\rho_a^o} & \frac{-(Z^o - Z_a)}{\rho_a^o} & 1 \\ \frac{-(X^v - X_a)}{\rho_a^v} & \frac{-(Y^v - Y_a)}{\rho_a^v} & \frac{-(Z^v - Z_a)}{\rho_a^v} & 1 \end{bmatrix} \quad (2.13)$$

$$x = \begin{bmatrix} \Delta X_a \\ \Delta Y_a \\ \Delta Z_a \\ \Delta c \delta \tau_a \end{bmatrix} \quad (2.14)$$

$$b = \begin{bmatrix} \text{observed PR}_a^e - (\rho_a^e + c \cdot \delta \tau_a - c \cdot \delta t^e + \text{dion}_a^e + \text{dtrop}_a^e) \\ \text{observed PR}_a^n - (\rho_a^n + c \cdot \delta \tau_a - c \cdot \delta t^n + \text{dion}_a^n + \text{dtrop}_a^n) \\ \text{observed PR}_a^o - (\rho_a^o + c \cdot \delta \tau_a - c \cdot \delta t^o + \text{dion}_a^o + \text{dtrop}_a^o) \\ \text{observed PR}_a^v - (\rho_a^v + c \cdot \delta \tau_a - c \cdot \delta t^v + \text{dion}_a^v + \text{dtrop}_a^v) \end{bmatrix} \quad (2.15)$$

$$v = \begin{bmatrix} v_a^e \\ v_a^n \\ v_a^o \\ v_a^v \end{bmatrix} \quad (2.16)$$

In general, least squares enable the  $x$  vector to be solved as

$$x = N^{-1} d \quad (2.17)$$

Where

$$\begin{aligned} N &= A^T A \text{ (or } A^T P_1 A) \\ d &= A^T b \text{ (or } A^T P_1 b) \end{aligned} \quad (2.18)$$

And  $P_1$  are the a-priori weights of the equations, with the pseudo-range typically either being given equal weights or being weighted with respect to elevation angle.

The full procedure employed by a receiver would be as follows (Bingley 2014):

- (i) For each satellite, calculate the satellite clock offset (in the satellite time frame) and the time of transmission (in the GPS time frame), from the information given in the broadcast ephemeris.
- (ii) For each satellite, calculate the satellite coordinates at the time of transmission (in the GPS time frame), from the information given in the broadcast ephemeris, and then calculate the computed pseudo-range, based on the approximate station coordinates and the satellite coordinates.
- (iii) Form the  $A$  matrix,  $b$  vector,  $N$  matrix,  $d$  and  $v$  vector, then solve for the  $x$  vector and update the approximate station coordinates.

In practice, steps (ii) and (iii) would then be repeated until the corrections to the approximate station coordinates are negligible.

The levels of plan and height accuracy can be calculated by using Gauss propagation of errors law (Bingley 2014).

$$\text{Accuracy} = \sqrt{(\text{satellite coordinate error})^2 + (\text{satellite clock error})^2 + (\text{ionosphere bias})^2 + (\text{troposphere bias})^2} \quad (2.19)$$

i.g.  $\sqrt{(1\text{m})^2 + (1\text{m})^2 + (3\text{m})^2 + (1\text{m})^2} = 3.5\text{m level of accuracy in plan} \quad (2.20)$

### 2.8.3 Differential GPS

When using a receiver in the reference station in known Cartesian coordinates, the reference station receiver uses full pseudo-range observation equations with the known coordinates(x, y, z) and the coordinates of the satellites -the geometric ranges to the satellites are solved. The difference of the observed pseudo-range and geometric range is the pseudo-range corrections at the reference station. The rate pseudo-range correction change is also defined. The corrections and rate of change are transmitted to the DGPS user receiver within range of the reference station. The vessel's DGPS receiver uses the corrections to improve its positioning solution (Groves 2013).

### 2.9 RTKLIB 2.4.3.

RTKLIB is an open source program developed by Akio Yasuda and Tomoji Takasu of the Tokyo University of Marine Science and Technology for DGPS processing. It can be used for logging, converting, downloading, streaming and processing of GNSS data from a variety of sources and computing position solutions. The part of RTKLIB ver.2.4.3 used in this research is the post-processing RTKPOST and RTKCONV for converting the raw data to Receiver Independent Exchange Format (RINEX). RTKLIB provide the solution types as follows:

- Single                      Single solution uses only data from one receiver to calculate its position.
- DGPS/DGNSS              This algorithm performs code-based differential GPS/GNSS. It does require a reference receiver.

- Fixed                    This algorithm assumes the receiver is stationary and then averages the whole measurement time to calculate the fixed position.
- Kinematic            This is the RTK algorithm. It uses carrier phase to calculate the position of a moving rover relative to the base station.
- Static                 This is also a carrier phase algorithm but it makes the assumption that the rover is stationary.
- PPP Kinematic       Precise Point Positioning (PPP) uses a very precise satellite clock and ephemeris data made available online 10-12 days after recording.
- PPP Static            PPP algorithm again, but which assumes a stationary receiver.
- Moving Baseline     RTK solution when the base station is not assumed to be stationary.

RTKLIB can be used in both real-time to generate GNSS solution or as in this thesis in the post processing.

The quality of the processed solutions is expressed by quality flags. A quality flag is as follows:

- Q=1            is fix solution
- Q=2            is float solution quality
- Q=4            is DGPS quality
- Q=5            is single quality solution

### **3 METHODOLOGY**

The measurements to be exploited were divided into three parts. First, a static measurement of both rover and base station. Second, a dynamic measurement where the rover is simulating ship movement by tilting the rover antenna only and the base station is static. The third part is a static measurement from the NYA1 reference station during the sun activity on 22 June 2015. The measurements were conducted at Svalbard using the positions:

- Rover station near Longyearbyen, Svalbard in position  $78^{\circ} 13'N - 015^{\circ} 24'E$
- Base station near Longyearbyen, Svalbard in position  $78^{\circ} 14'N - 015^{\circ} 23'E$
- NYA1 Reference Station in Ny-Ålesund, Svalbard in position  $78^{\circ} 55'N - 011^{\circ} 51'E$

#### **3.1 Equipment**

Leica GS10 geodetic dual frequency receiver with 150 channels able to track signals from GPS, GLONASS, Galileo and BeiDou were used at both rover and base sites. The receivers were connected to a Leica AS10 antenna and mounted on a Leica CTP101 Wooden Tripod (see Appendix A for further specifications). The angle of the legs of the tripods was set to about 45 degrees and supported with stones to avoid vibrations.

Manfrotto 804RC2 tilt head normally used by cameras and with the possibility to tilt 90 degrees was used to tilt the rover antenna.

One small screw transition between the antenna and the tilt head and a large screw transition between the tilt head and the tripod were produced by the workshop of the University of Nottingham.





**Figure 3.1** Photo at Svalbard of the rover station with the Manfrotto tilt head and screw transitions to the left and the base station to the right.

Trimble NETR8 dual frequency receiver able to track signals from GPS and GLONASS and ASH701073.1 antenna in NYA1 Reference Station was used during sun activity (see Appendix B for further specifications).

### **3.2 Test Measurement**

The methodology of ensuring correct measurement on Svalbard was to conduct a test measurement at the University of Nottingham to be conducted 5 June and 10 June. The topics were:

- Learning to set up the Leica receivers, antennae and tripods
- Program for receiving GPS, GLONASS, Galileo and BeDou raw data
- To test the Manfrotto tilt head and the screw transitions
- To collect the recorded data and control of the data
- To produce the customs declaration document
- To control all components needed on Svalbard

### **3.3 GNSS Combinations**

The GNSS combinations to be further explored are the pseudo-range combinations and DGPS:

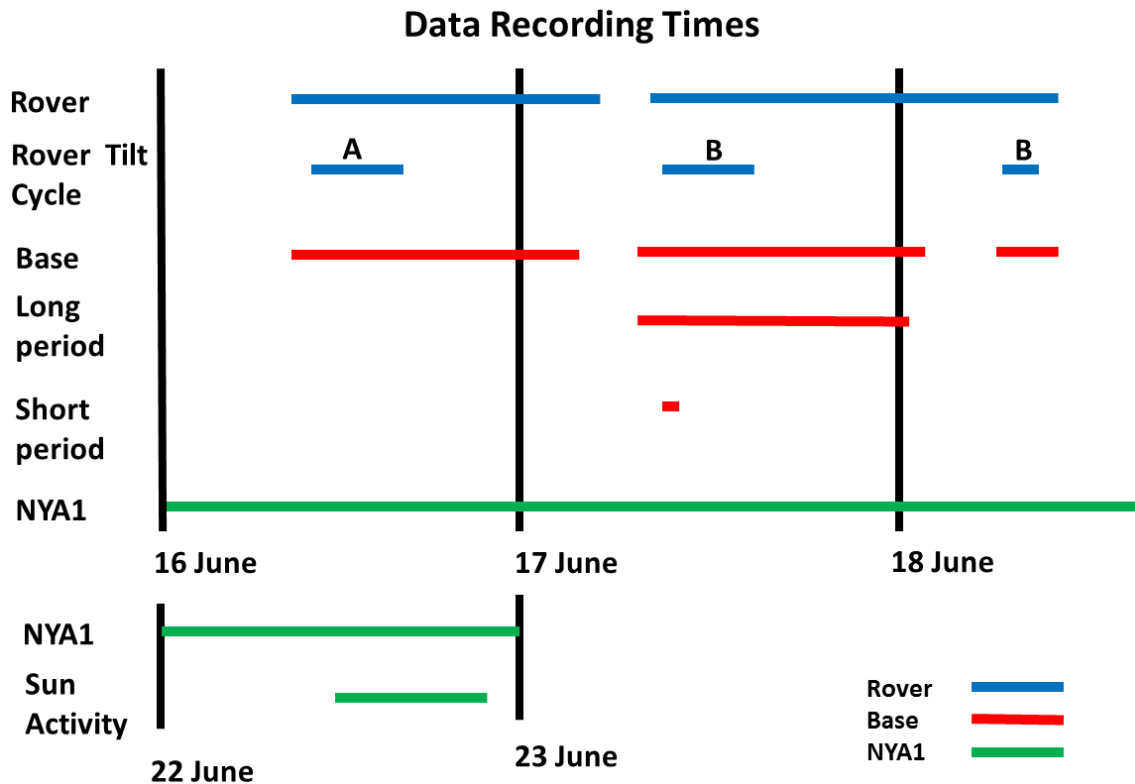
- GPS Single receiver using L1 only
- GLONASS Dual receiver
- GPS Dual receiver using L1 and L2
- GPS+GLONASS combined
- DGPS

The GPS Double Difference Kinematic approach was used to define the true positions of the Rover and Base stations antennae using NYA1 Reference Station. Kartverket, the Norwegian Mapping Authority, an organisation operating the NYA1 specified the true position of NYA1 with more decimals than available on the information site of NYA1 on the internet (Kartverket 2015).

### **3.4 Data Recording**

#### **3.4.1 Data Recording Times**

The planned recording time of Leica receivers was 48 hours continuous recording to ensure two ground repeats of GPS. However, due to the rules of the restricted area at Svalbard Satellite Station all personnel had to leave the area at the end of working hours. The procedure to ensure the longest recording time during the chilly night was install fresh batteries into the Leica receivers at the end of working hours and to check the receivers in the morning the-next day.



**Figure 3.2** An overview of the data recording times of rover station, base station and NYA1 reference station in addition the period of the tilt cycle, long period, short period and sun activity

### 3.4.2 Data Recording Files

Leica receivers were configured to record raw data every second in Receiver Independent Exchange Format (Rinex) of GPS, GLONASS, Galileo and BeiDou satellite signals. The recordings of Galileo and BeiDou satellites were by request from the University of Nottingham. Only the GPS and GLONASS data was used in the research. The raw data files periods in GPS Time consisting of observation data files and navigation message files collected from Leica receivers are:

- Rover receiver            16 June from 0845 - 2359
- 17 June from 0001 - 0619 and 0925 - 2359
- 18 June from 0001 – 1029

- Base receiver                    16 June from 0845 - 2359  
                                           17 June from 0001 - 0311 and 0730 – 2359  
                                           18 June from 0001 – 0201 and 0745 – 1050

The raw data files periods in GPS Time consisting of observation data files and navigation message files of GPS and GLONASS only collected from NYA1 Reference Station Receiver (IGS 2015).

- NYA1 Reference Station        16 June from 0001 – 2359  
                                           17 June from 0001 – 2359  
                                           18 June from 0001 – 2359  
                                           22 June from 0001 – 2359

The raw data was collected and copies were taken as backup when the receivers were restarted with fresh batteries at the end of the measurements. Photos were made, and stop watch and notes were used to document the measurements.

### **3.5 Static Receiver**

#### **3.5.1 Long Period**

The scope of the long period measurement of one static receiver is to analyse the pseudo-range position solution of the GNSS combinations with regards to accuracy, precision, number of tracked satellites, their numbers, SNR, skyplots, HDOP and VDOP during a long period without interference. The longest continuous period of recorded data from Svalbard was recorded at the base station and was selected according to this analysis.

Rinex 2 raw data from base station was converged and used in this part of investigation.

The long period of 16 hours 30min is on 17 June at 0730 - 2400 GPST.

### **3.5.2 Short Period**

The scope of the short period measurement of static receivers is to analyse the same details as those of long period. However, the short period was selected using the Trimble GNSS planning online to detect a period with few GPS and GLONASS satellites and high HDOP and VDOP. The numbers of GPS and GLONASS satellites in the short period are low.

Raw data from base station was converged and used.

The short period of 18 min and 30 seconds is on 17 June from 10:19:30 to 10:38:00 GPST.

### **3.6 Ship Movement Simulation**

GNSS antennae are normally mounted on the mast of the vessel and moves and tilts at the same pace as the ship's pitch and rolls. Ship GNSS antennae are not static but dynamic. To simulate the maritime antenna movement the Manfrotto tilt head was acquired and screw transitions made. The scope of the ship movement simulation is to investigate the effect of tilt movements in a known position. The change of antenna centre is about 7 cm from 15 degrees tilt to the West to 15 degrees to the East. The change is about 12 cm with 30 degrees tilt movements. The tilt head was located on the rover station between the antenna and the tripod.

### **3.6.1 Ship Movement Cycle**

The tilt cycle A and B was used. The ships movements are determined by the structure and size of the vessel, sea states, degree of turn and the ships' stabilizer. However, roll keels and fin stabilizers cannot be used in an area of ice. The tilt angles 15 and 30 degrees of the rover antenna were selected to challenge the GNSS systems.

Tilt Cycle A:

- Before 0 degree tilt for 2 minutes
- Tilt 15 degrees to West for 2 minutes
- Tilt 15 degrees to East for 2 minutes
- Moving tilt back and forth from 15 degrees West to 15 degrees East every 10 seconds for a duration of 2 minutes.
- After 0 degree tilt for 2 minutes

Tilt Cycle B: Same as tilt Cycle A but in addition to A after the moving tilt of 15 degrees:

- Moving tilt back and forth from 30 degrees West to 30 degrees East every 10 seconds for a duration of 2 minutes.

### 3.6.2 Ship Movement Procedure

The procedure conducted of the tilt cycle was:

- Stay below the rover antenna's view at all times
- Cover completely the antenna for 15 seconds before each part of the tilt cycles to be able to identify the tilt cycles in the processed outputs
- Stop watch used to control the execution of cycle
- The top tilt function on the tilt head closest to antenna was used
- Time notation



**Figure 3.3** Rover Station Manfrotto tilted 15 Degrees to West before the measurements started.

### 3.6.3 Ship Movement Cycle Times

The times in GPST of the conducted ship movement cycles are:

- 16 June
  - 1A from 0957 - 1002
  - 2A from 1100 - 1105
  - 3A from 1200 - 1210
  - 4A from 1300 - 13010
  - 5A from 1401 - 14011
- 17 June
  - 1B from 0921 - 0933
  - 2B from 1020 - 1042
  - 3B from 1132 - 1142
  - 4B from 1231 - 1241
  - 5B from 1330 - 1341
- 18 June
  - 6B from 0814 - 0825
  - 7B from 0915 - 0927

The tilt cycle 2B was conducted at the same time as the short period and was selected for closer analysis.

### 3.7 Sun Activity

The scope of the sun activity part is to investigate how sun activity affects the GNSS ability to perform the positioning service in the arctic area. There was low solar activity during research measurements on Svalbard. However, the Trimble GNSS planning online software and Kartverket did register sun activity on 22 June (Trimble 2015) (Kartverket 2015). The peak activity at Svalbard was on 22 June at 2030. A normal activity closest in time happened at 2055.

Rinex 2 raw data of GPS and GLONASS of 22 June 2015 was downloaded from IGS (IGS 2015).

Time periods in GPST selected for analysis are:

- Sun activity                      22 June              from 2027 - 2032
- Normal activity                  22 June              from 2052 - 2057



## **3.8 Data Analysis Techniques**

### **3.8.1 GNSS Planning Software Tool**

The methodology to discover periods of interest for the Trimble GNSS planning online software tools were used. The short and long period static test was selected by using Trimble planning tool. Total 14 days period including the days of measurements were investigated including satellite library, expected HDOP and VDOP values, skyplots, visibility of satellites, elevation of satellites, number of satellites and Iono information. The sun activity period was discovered on Trimble planning tool two weeks after the measurements were finished.

### **3.8.2 RINEX Raw Data Extraction**

The methodology to ensure that the post processing program only used the Rinex 2 data specified to the GNSS combination to be processed the converging processing tool RTKCONV ver.2.4.3 was used. The Rinex 2 raw data of rover, base station and NYA1 was converged to:

- Converged Rinex 2 GPS Single L1 data
- Converged Rinex 2 GPS Dual L1+L2 data
- Converged Rinex 2 GPS+GLONASS data
- Converged Rinex 2 GLONASS data
- Converged Rinex 2 DGPS data

The converged data was used in the post processing production.

### **3.8.3 Data Analysis Software Tool**

The converged Rinex 2 data from the Leica receivers and NYA1 were post processed in RTKLIB 2.9.3 software tool using the RTKPOST. The settings and plots were organized and stored.

The elevation angle mask 15 degree was used to reduce multipath effect.

## **3.9 Location Of The Site**

### **3.9.1 Determination of Site**

To select the site of the measurements, the methodological criteria were as follows:

- To be at the same latitude as in Svalbard area and the NEP from about 71 to 83 degrees north
- The possibilities for transport back and forth between Nottingham and the location
- On Norwegian territory
- Open sky to the satellites
- Possibility of electric power
- Safety of equipment
- Place to be, eat and stay
- Safe from being attacked by polar bears

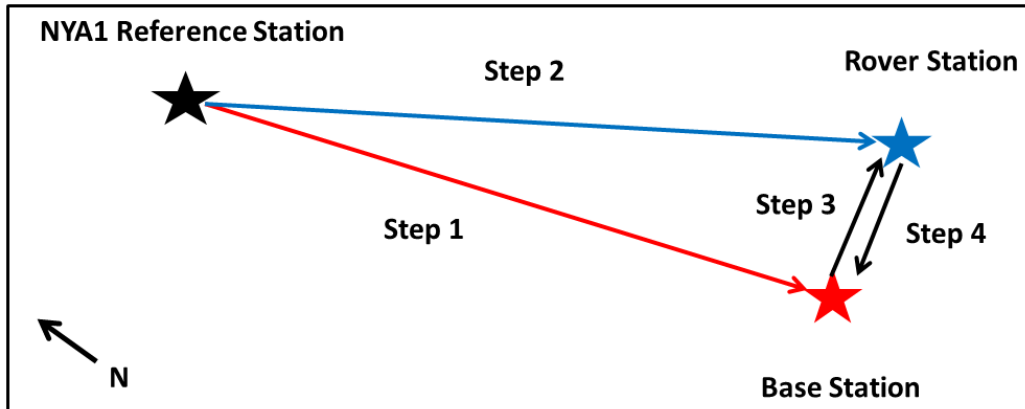
Locations at the North Cape in Norway, Bear Island, Hopen Island, Ny-Ålesund at Svalbard and Longyearbyen at Svalbard were investigated. Longyearbyen at Svalbard was chosen over Ny-Ålesund to be able to use the NYA1 reference station at Ny-Ålesund. The application for access to the restricted satellite ground station area KSAT Svalbard Satellite Station (Svalsat) was approved in March.



**Figure 3.4** KSAT Svalbard Satellite Station at Svalbard (Extracted from: [www.ksat.no](http://www.ksat.no))

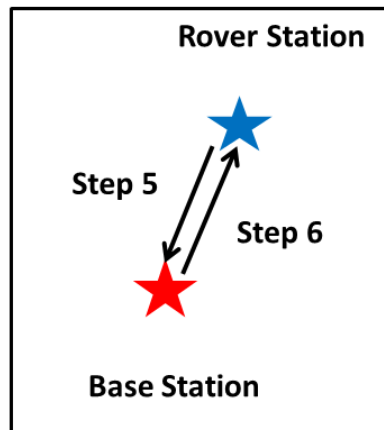
### 3.9.2 True Position of Rover and Base Station

Methodology used to define true position of rover and base station was the double difference kinematic approach following the steps:



**Diagram 3.1** Diagram of step 1 to 4 of the DD Kinematic approach

- Step 1: DD kinematic with true position of NYA1 reference station as base station and the research base station as rover. Baseline length 110.1 km.
- Step 2: DD kinematic with true position of NYA1 reference station as base station and the research rover station as rover. Baseline length 110.2 km.
- Step 3: DD kinematic with the position from step 1 of research base station as base station and research rover station as rover. Base length 61.34m.
- Step 4: DD kinematic with the position from step 2 of research rover station as base station and research base station as rover. Base length 61.34m.

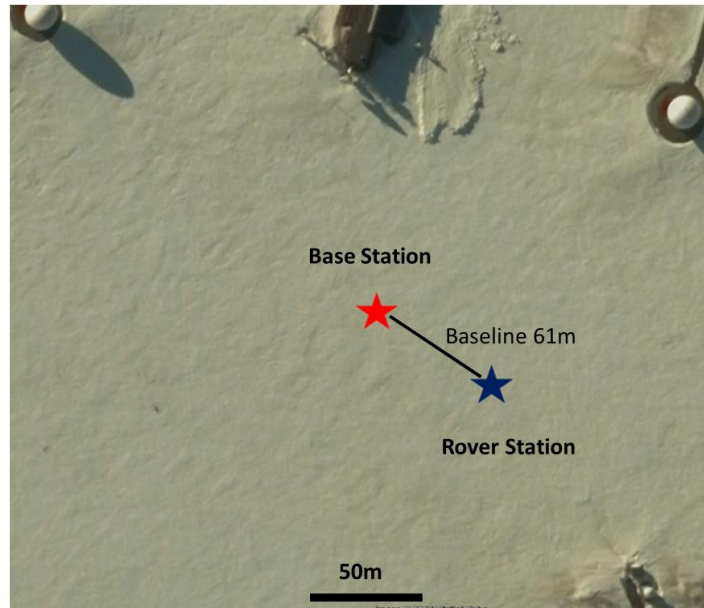


**Diagram 3.2** Diagram of step 5 and 6 of the DD Kinematic approach

- Step 5: DD kinematic with the position from step 3 of research rover station as base station and research base station as rover. Base length 61.34m.
- Step 6: DD kinematic with the position from step 5 of research Base station as base station and research Rover station as rover. Base length 61.34m.



**Figure 3.5** Location of NYA1 reference station and base and rover stations in map of Svalbard



**Figure 3.6** Location of base station and rover station at KSAT Svalbard Satellite Station and the 4 obstacles

Distance and elevation to the top point of the 4 obstacles around the rover and base station are:

- Base station: Antenna upper left                      distance 215m - angle 6 degrees
- Building top                                              distance 124m - angle 4 degrees
- Antenna upper right                                      distance 178m - angle 5 degrees
- Antenna bottom right                                      distance 193m – angle 4 degrees
- Rover station: Antenna upper left                      Distance 284m – angle 6 degrees
- Building top                                              Distance 188m – angle 4 degrees
- Antenna upper right                                      distance 165m – angle 5 degrees
- Antenna bottom right                                      distance 123m – angle 4 degrees



**Figure 3.7** Photo of rover station to the left and base station to the right at Svalbard Satellite Station at the beginning of the measurements

### **3.10 Presentation Of Results**

Firstly, to establish the true position of rover and base station the output of the last two steps of the double differencing process will be plotted in scatter plots using the average latitude and longitude and height as origin. The position of NYA1, rover and base station will be plotted in Google maps. The zoomed in positions of rover and base stations at Svalbard Satellite Station will be plotted in Google Earth. Diagram of the three sites gives an overview.

Further, the long and short period static tests and the ship moving test are studied in detail of all the GNSS combinations by looking at their absolute accuracy and precision values using the true positions of rover and base station as origin in the scatter plots. The GNSS combination's true accuracies and precisions in latitude, longitude and height will be calculated and put into tables. The sun activity study of GPS single L1 and GPS+GLONASS will be studied in detail using the true position of NYA1 as origin in the scatter plots. Tables of the absolute accuracy and precision will be calculated and used in the comparison.

The geometry DOP, HDOP and VDOP and a number of satellites will be put in same plot in the study of their relations. Skyplots of elevation and direction of the satellites of the two GNSS systems show their similarities and differences. Multipath, visibility of satellites and pseudo range residuals plots will also be presented in the research.

SNR plots of GPS and GLONASS to be used in the investigation of the systems in the sun activity and static measurements.

In the study of ship movement tables of each GNSS combination and the tilt cycle 2B are calculated and used in the comparisons.

### **3.11 Research Design Issues And Limitations**

The static long period was selected because it was the longest continuous recorded data and not the 48 hours duration as planned. The danger of polar bear attacks and KSAT Svalbard Satellite Station regulations of the restricted science area caused the Leica receiver batteries to run flat during the night. It has to be mentioned that there had been 4 polar bear attacks at Svalbard prior to the measurements, but none in Longyearbyen or in the Svalsat area.

The lowest number of GPS satellites visible decided the time and duration of static short period and lasted for only 18 minutes and 30 seconds. The ship movement simulation cycle 2B with duration of 22 minutes was conducted during the short static period. The tilting antenna cycle 2B was selected for further investigation in order to test the GPS and GLONASS combinations of relative few satellites, high HDOP and VDOP and a moving antenna. In a 24 hour period perspective, the 22 minutes of moving cycle 2B is a snapshot of the GPS and GLONASS systems and does not represent the systems in a long term.

The sun activity period is short because the peak of sun activity was short.

The GNSS combinations were post processed from data of survey grade receivers to be able to compare the combinations according to an absolute true position. The civil vessels use real maritime GNSS equipment from different manufacturers and characteristics to measure and process in real time. Post-processing the GNSS solutions has advantages over real time solutions. The algorithm can be run both forwards and backwards in time



and thereby smoothen the solution. It is also possible to use information of ionospheric, tropospheric, satellite ephemeris, and satellite clock corrections. To limit these advantages the "Forward" and "Broadcast" functions were used in RTKLIB.

The location of the measurements was selected according to the criteria of location. It is on land at altitude 463m and not on board a vessel at sea level with multipath from superstructure, the sea, mixed sea and ice and ice only. The multipath of rover and base station are from snow and buildings at distance.

The date of measurements was at the beginning of the season in NEP and the research does not cover the complete season of NEP.

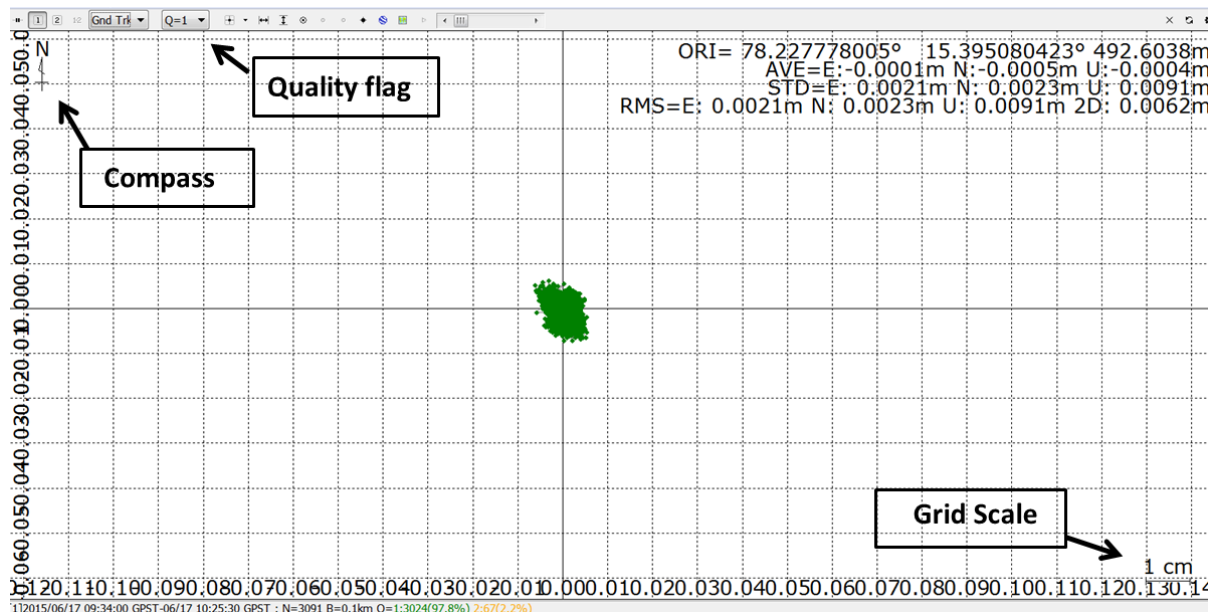
The elevation angle mask of 15 degrees to reduce multipath effect limits the number of satellites in view. This also affects the robustness of the GNSS systems particularly during the ship moving simulation research.

The tilt angles of 15 and 30 degrees of the rover antenna represent large ship movements, not ship movements in calm seas.

## 4 RESULTS AND DISCUSSION

### 4.1 True Position Of Rover And Base Station

To define the true positions of base and rover station, the steps in DD Kinematic described in the methodology chapter were followed. The result of step 5 which uses rover station as base and base station as rover and base length 61.34m is showed in figure 4.1.



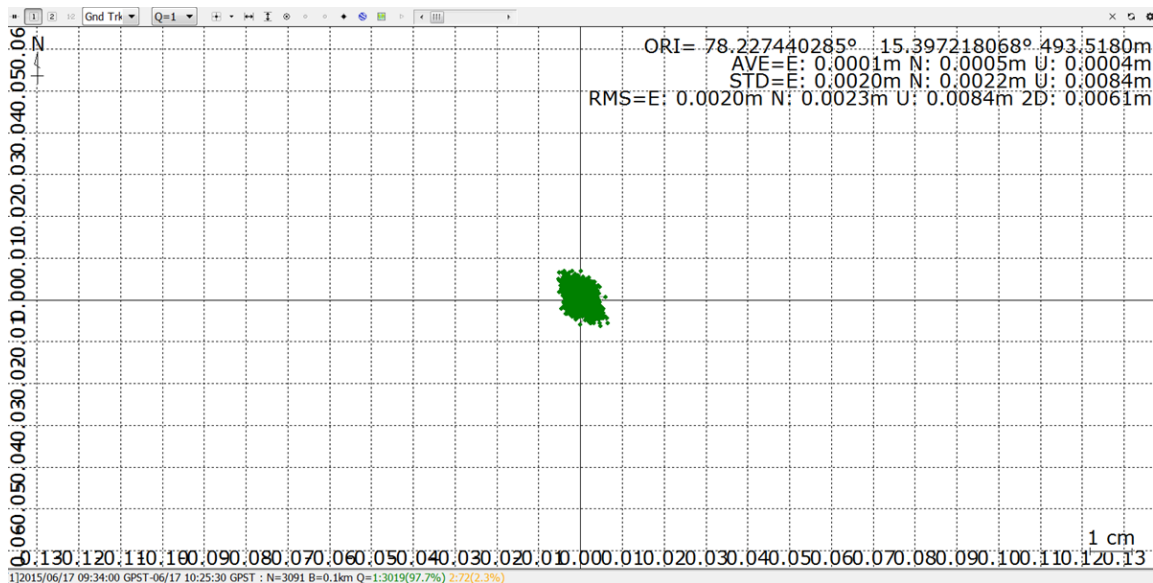
**Figure 4.1** Scatter plot of DD Kinematic defining the true position of base station.

The RTKLIB scatter plot uses a quality flag to indicate the quality as highlighted in figure 4.1. Q=1 is fix quality. Further, it presents the compass at the upper left corner and the scale of the plot bottom right. The scatter plot in figure 4.1 defines the average position of fix solutions as origin and defines the true position of the base station. The height used in the research is the ellipsoidal height in meter.

The true position of base station is:

78.227778005°N – 15.395080423°E - Height 492.6038m

The result of step 6 which uses the true position of base station as base and rover station as rover and base length 61.34m is showed in figure 4.2.



**Figure 4.2** Scatter plot of DD Kinematic defining the true position of rover station.

The average position of quality 1 is the origin and the true position of rover station is:

78.227440285°N - 15.397218068°E - Height 493.518m

The true position of rover and base station represents the truth in the research and in the comparison of GNSS combinations in long and short periods as well as in the ship movement simulation parts.

## 4.2 Long Period

### 4.2.1 Accuracy and Precision

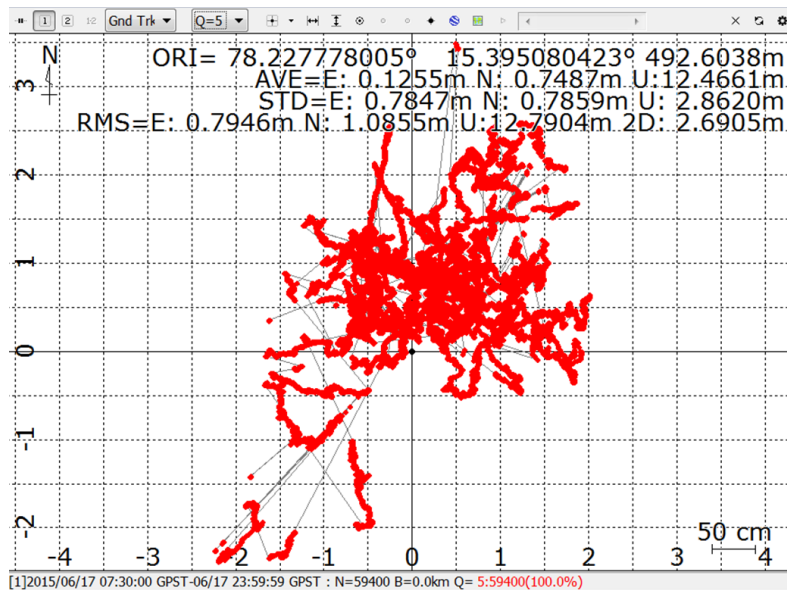
The GNSS combinations: GPS Single, GLONASS, GPS Dual, GPS+GLONASS and DGPS have been processed and their absolute accuracy and the precision set into table 4.1.

Long Period Base Station	Accuracy (m)			Precision (std) (m)		
	N	E	U	N	E	U
GPS Single L1	0.74	0.12	12.45	0.79	0.78	2.86
GLONASS	0.41	0.92	0.32	2.37	1.96	7.49
GPS Dual L1+L2	0.61	0.15	0.95	0.58	0.64	2.41
GPS+GLONASS	0.55	0.22	0.79	0.61	0.53	2.11
DGPS	0.05	0.02	0.28	0.47	0.34	1.71

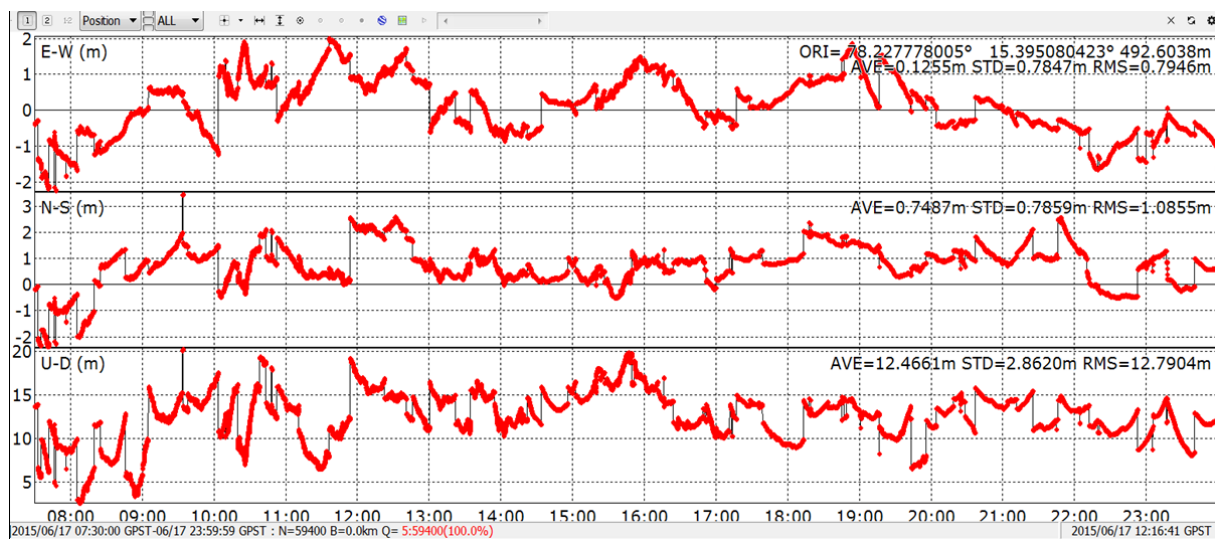
**Table 4.1** The table is the accuracy and precision as performed by the GNSS combinations in the long period at base station. Green is best value in the row and red is the lowest performance.

The accuracy tables show the absolute accuracy. The average position of the measurements is calculated as accuracy in reference to the true position of base station. The precision is the scattered epoch positions of one standard deviation (std) in reference to the average position. Both accuracy and precision are presented in meters.

GPS Single using only L1 cannot conduct 'ionospheric free' pseudo-range. The combination has the lowest accuracy in North direction but is still below 1 meter. The GPS HDOP during the research was very good due to the good spread of satellites in all directions. Due to the inclination angle of the equator of 55°, the spread of satellites in the arctic area is in the horizontal area and above making the HDOP value very good.

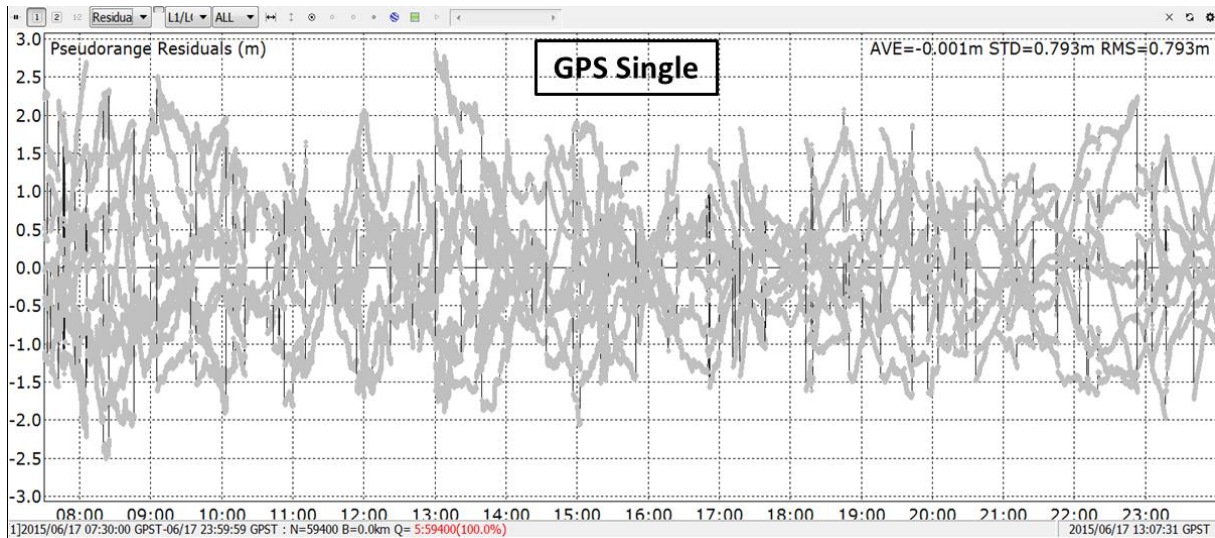


**Figure 4.3** GPS Single plan scatter plot from base station in the long period. Q=5 means single pseudo-range quality. Grid scale is 50 cm. The X axis is West/East and Y axis is North/South in meters.



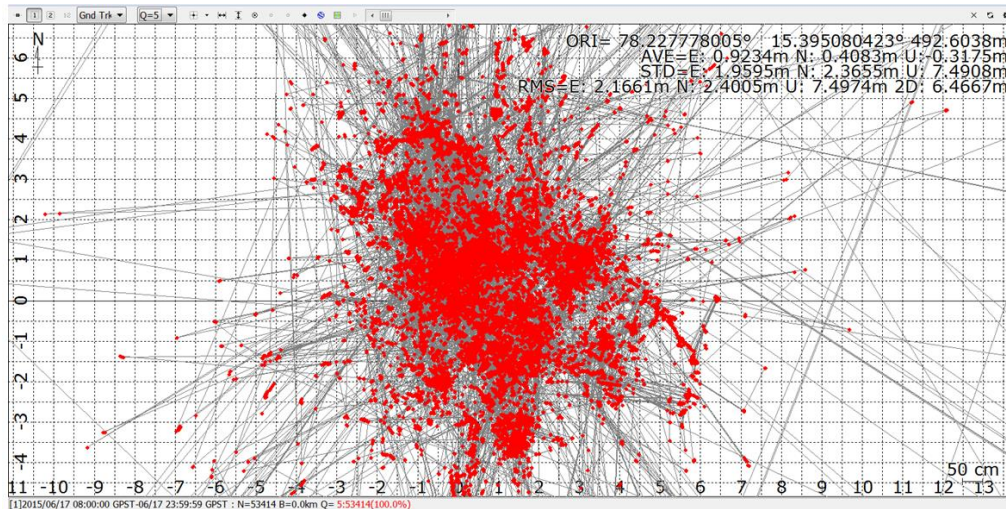
**Figure 4.4** GPS Single position plot in time series from base station in the long period. The top plot is the East-West plan direction. The middle plot is the North-South plan direction and the bottom is the Up-Down direction. X axis is GPS Time and Y axis is true accuracy in meters.

Due to no GPS satellites at very high angle and above the receiver the VDOP value is similar poor. This affects the accuracy in height where GPS Single by far had the worst accuracy of 12.4m (table 4.1 and figure 4.4). According to Dr Bingley, the thumb rule of relation between plan accuracy and height accuracy is that the height accuracy is about two and a half value of the plan accuracy (Bingley 2015). At high Latitude as 78°N this rule of thumb cannot be used with GPS Single receivers.



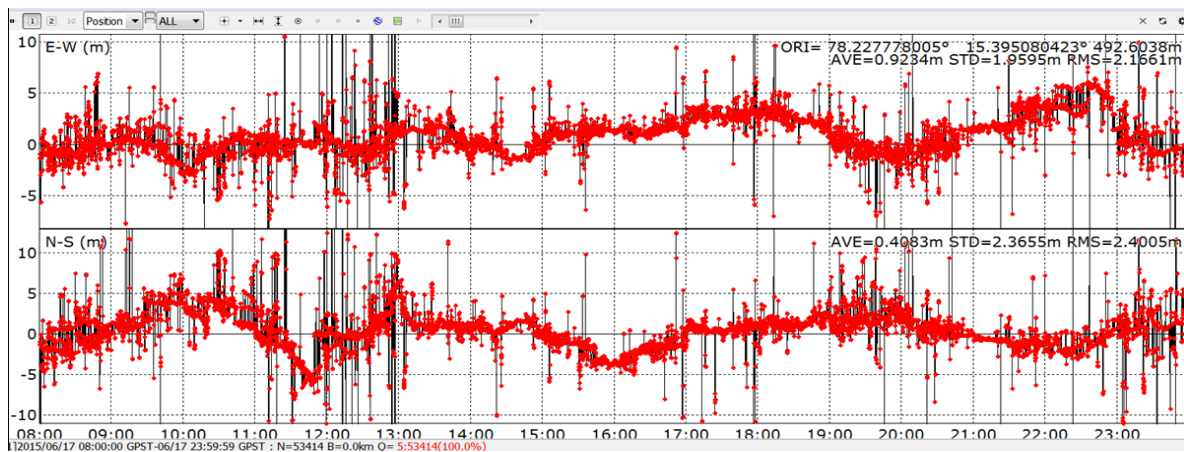
**Figure 4.5** Plot of the GPS Single pseudo-range residuals in times. X axis is the GPS time and Y axis is the residuals in meter.

Pseudo-range measurement residual is the difference between the expected measurement pseudo range and the observed pseudo-range. The pseudo-range residuals is the rest of systematic error and biases not counted for.



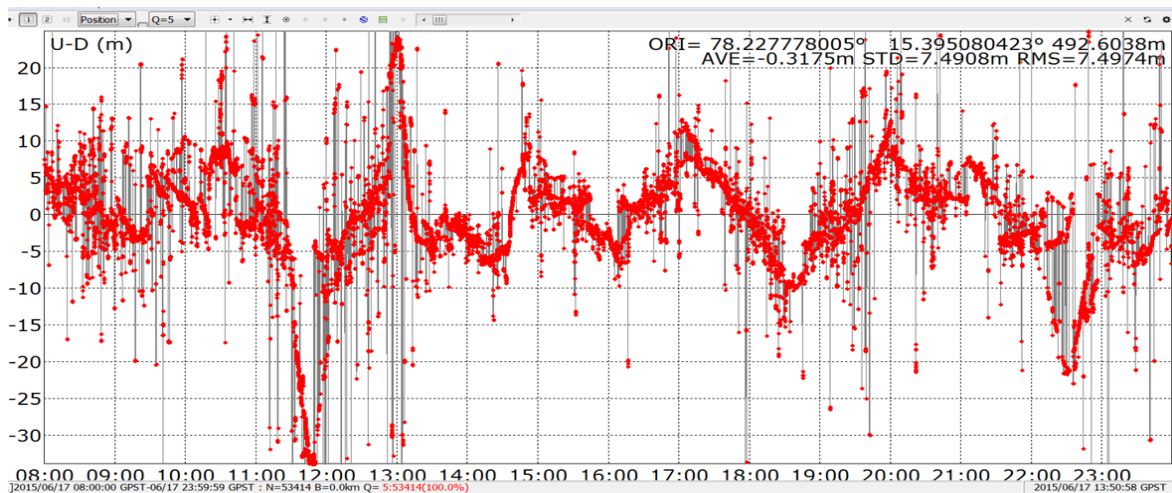
**Figure 4.6** GLONASS plan scatter plot from base station in the long period. Grid scale is 50 cm. The X axis is West/East and Y axis is North/South in meters.

GLONASS has the lowest accuracy in East and the lowest precision in both North, East and in Up directions. The scatter plots of GLONASS seem much more scattered and more disturbed than those from the GPS combinations (figure 4.6 and 4.7).



**Figure 4.7** GLONASS plan position plot in time series from base station in the long period. The top plot is the East-West plan direction. The bottom is the North-South plan direction. X axis is GPS Time and Y axis is true accuracy in meters.

Factors such as less quality of the satellite clocks, less accurate spatial coordinates due to no global coverage of the ground segment and the use of FMDA may be the reason. The receiver must acquire the GLONASS signal and track the code phase. The GLONASS satellites travel slightly faster than GPS satellites and when the satellite comes towards or directly from the receiver the transmitted frequency is changed at ground level due to the Doppler effects. Satellites movement to the side create less Doppler effects. The GLONASS receiver uses the satellites frequencies to identify the satellite, and when the frequencies are also changed due the satellite movements it makes it harder for the receiver to acquire GLONASS satellite signals. The number of satellites used in each epoch changes much more in the GLONASS system than in GPS.

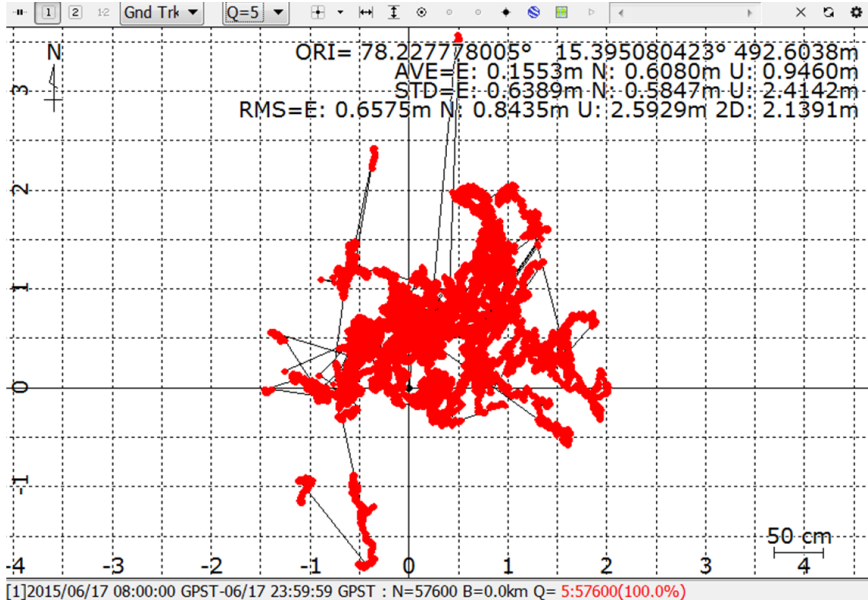


**Figure 4.8** GLONASS height plot from base station in the long period. The X axis is GPS Time and Y axis is accuracy in meters.

Concerning height (figure 4.8), GLONASS has better accuracy than GPS due to the higher altitude of GLONASS satellites than GPS satellites. Satellites above the receiver improve the VDOP and height accuracy.

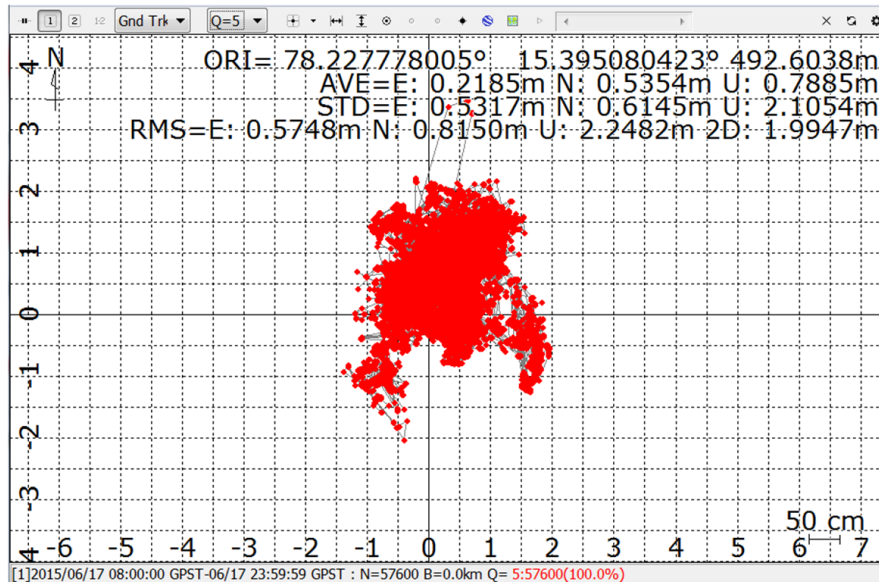


Dual GPS receivers share the same HDOP and VDOP values as GPS Single. Dual receivers have the ability of 98% reduction most influential bias by conducting 'ionospheric free' pseudo-ranges. The plan and height accuracy and precision are better than GPS Single solutions.



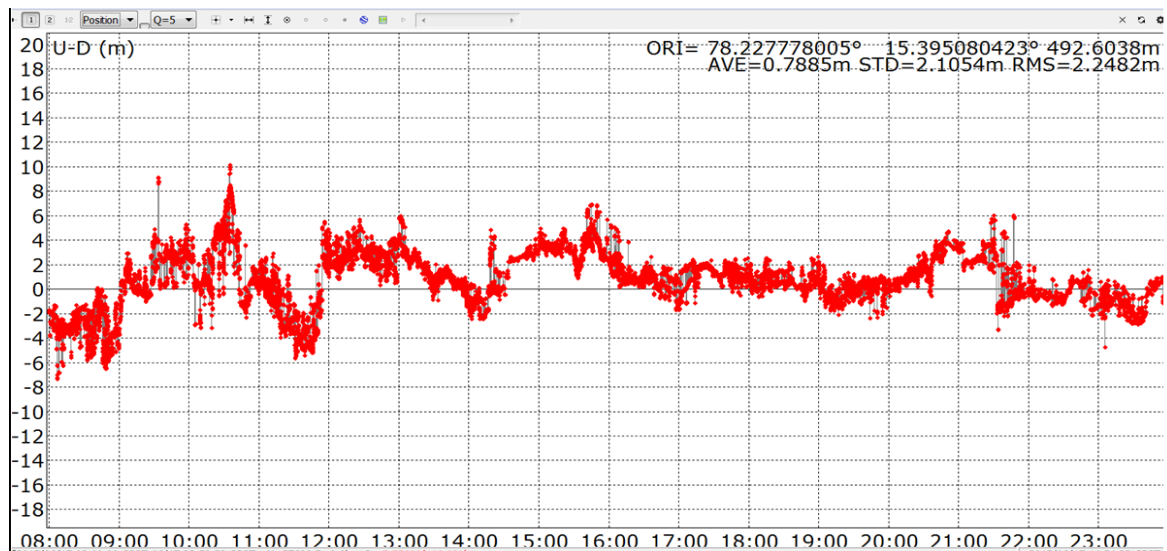
**Figure 4.9** GPS Dual plan scatter plot. Grid scale is 50 cm. The X axis is West/East and Y axis is North/South in meters.

The most interesting combination is the GPS+GLONASS due to the fact that it combines the two GNSS systems. As we can see from table 4.1 and figures 4.6 the GLONASS had in general the lowest performance in accuracy and precision. How can GLONASS improve the GPS solutions?



**Figure 4.10** GPS+GLONASS plan scatter plot from base station in the long period. Grid scale is 50 cm. The X axis is West/East and Y axis is North/South in meters.

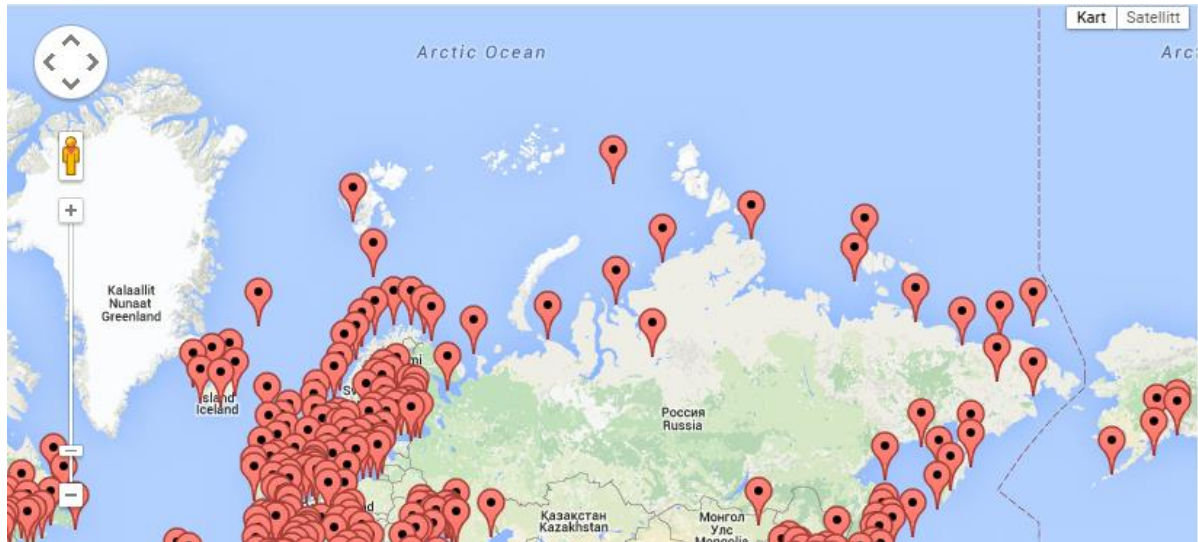
Let us omit the DGPS and look at table 4.1 and the pure stand-alone pseudo-range combinations. The GPS+GLONASS combination got the best precision in East and Up. In North directions the accuracy is better than both GPS Dual and GPS Single. In East direction the accuracy is better than GLONASS but was very close to those of GPS combinations. In Up direction the accuracy was better than both the GPS combinations. Finally, the precision in North was better than GPS Single and GLONASS. Of the six values, the combined combination performed best in 2, second best in 3, third best in one, no value being the worst. The values of GPS+GLONASS are very good with only one exceeding 1 meter.



**Figure 4.11** GPS+GLONASS height plot from base station in the long period. The X axis is GPS Time and Y axis is accuracy in meters.

The reason of the good performance in plan and height accuracy and precision, is the ability of using more satellites which increases the HDOP and VDOP. The receiver can select more signals, conduct 'ionospheric free' pseudo-range, mask signals with low accuracy or multipath and still have enough satellite signals to calculate the position solution. Just to remove low accuracy signals improves the solution. The receiver can select satellites in favourable constellations e.g. use mostly GPS satellites, but add GLONASS satellites with higher altitude. The GPS+GLONASS combination has the ability to exploit the good quality of each of the two GNSS systems, suppressing the bad sides. To put it simplistically, it may employ the GPS Dual solution in plan and GLONASS solution in height. Other's research has experienced the same improved solutions. According to Meng the improvement in positioning solutions by an integrated system of GPS and GLONASS was demonstrated with the data collected from Humber Bridge trials (Meng 2002).

Differential GPS has the best performance in accuracy and precision. It is widely used by civilian vessels in coastal and harbour areas. However, the DGPS is not a stand-alone pseudo-range approach as it receives and uses transmitted corrections from a reference station.



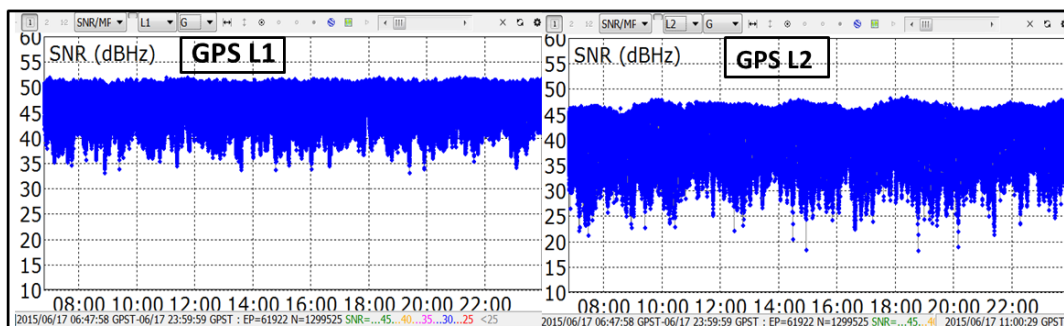
**Figure 4.12** Map of all IALA DGPS Reference Stations and beacons (GNSS Pro 2015).

The coverage area of DGPS is limited in the NEP as shown in figure 4.12. The Russian part of NEP has few reference stations. Manufacturers and organisations as: Sokkia, Veripos, Terrastar, Topcom, IGS and others implement multi GNSS in reference station equipment.

The assessment from the hypothesis that differential corrections can be received in some area of NEP proves to be correct.

### 4.2.2 Signal-to-Noise-Ratio

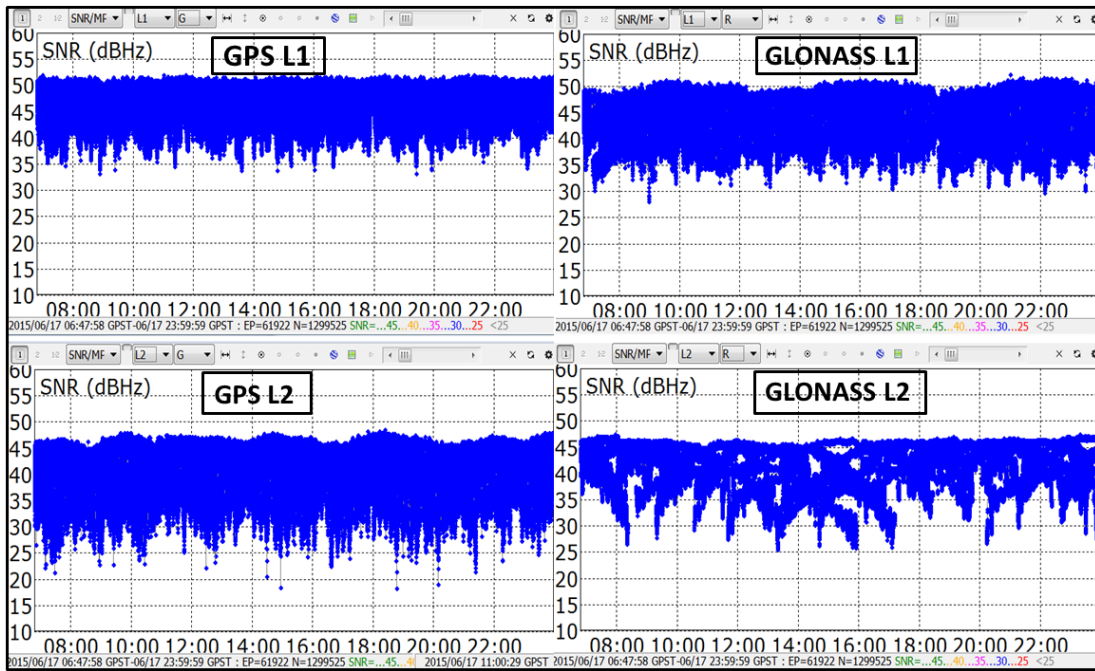
The value of SNR is very important for the receiver to be able to acquire the GNSS signals hidden in the background noise. SNR value is a product of power of the signal when it leaves the satellite, attenuation of the signal travelling between satellite and receiver, the elevation of the satellite from the observer and the quality of the receiver. The most influential factor is the elevation. The degree of attenuation also depends on the frequency. Higher frequency (L1) has less attenuation than lower frequency (L2).



**Figure 4.13** Plots of SNR of GPS L1 to the left and GPS L2 to the right. The X axis is the GPST and the Y axis is the SNR in dBHz.

The SNR values of GPS L1 are in general higher than GPS L2 (figure 4.13). GPS L1 starts around 35 dBHz and has a continuous and quite stable top level around 52 dBHz. GPS L2 starts around 25 dBHz which is about 10 dBHz lower than GPS L1. GPS L2 has a variable top level around 47 dBHz which is about 5 dBHz lower than GPS L1.

According to GPS.GOV "L2C broadcasts at a higher effective power than the legacy L1 C/A signal....." (GPS 2015). Even so, the received SNR in the research in Arctic is lower for L2 than for L1 due to the factors which affects the SNR.



**Figure 4.14** Plots of SNR of GPS L1 upper left corner, GPS L2 bottom Left, GLONASS L1 upper right and GLONASS L2 bottom right. The X axis is the GPST and the Y axis is the SNR in dBHz.

The SNR values of GLONASS L1 are in general higher than GLONASS L2 and GPS L2 but slightly lower than GPS L1 (figure 4.14). GLONASS L1 starts around 32 dBHz which is about 3 dBHz lower than GPS L1 with a variable top level around 50 dBHz which is about 2 dBHz lower than GPS L1. GLONASS L2 starts around 27 dBHz which is about 2 dBHz higher than GPS L2 and about 10 dBHz lower than GLONASS L1. GLONASS L2 has a variable top level around 47 dBHz which is about the same as GPS L2 and about 3 dBHz lower than GLONASS L1 and about 5 dBHz lower than GPS L1.

A general comparison of the satellites' signals SNR from research Base Station is:

- GPS L1 has the highest SNR
- GLONASS L1 has the second highest SNR
- GLONASS L2 has the third highest SNR
- GPS L2 Has the lowest SNR only slightly lower than GLONASS L2

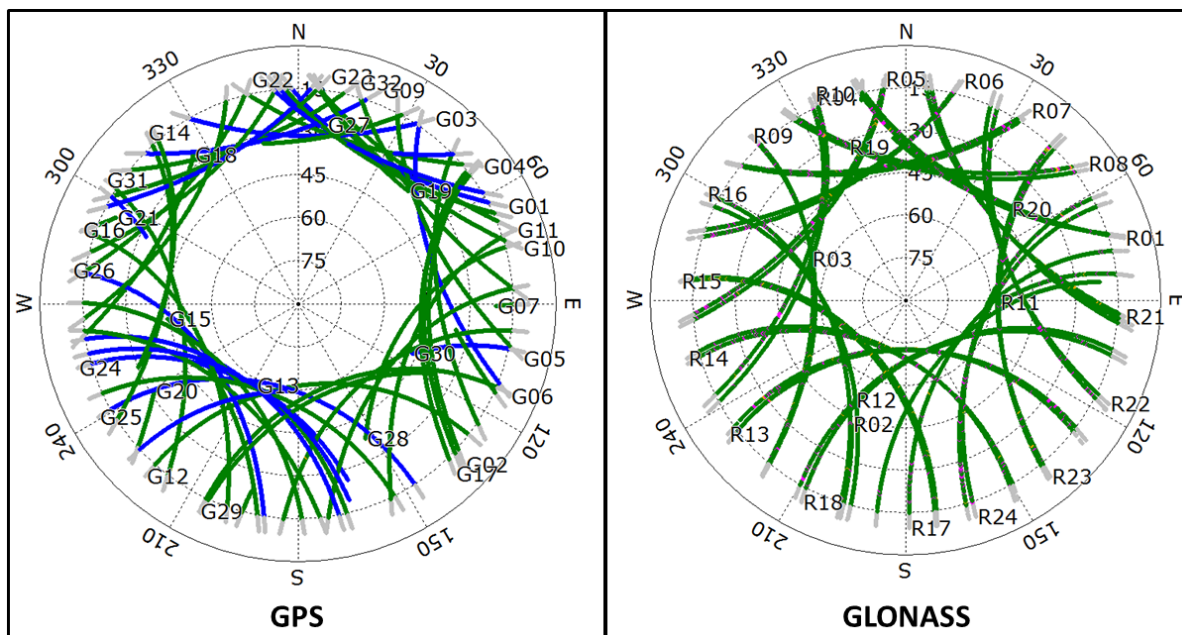
In multi GPS and GLONASS receiver, the receiver is able to exploit all four signals and their SNRs.

The hypothesis of the research in chapter 1, that the SNR of GLONASS signals are higher than GPS signals due to the higher altitude is partly wrong as GPS L1 has the highest SNR, and partly correct as GPS L2 has the lowest SNR.

### **4.2.3 Skyplot**

Skyplot is a plot of the view to satellites from the observer. The observer is in origin and the directions to the satellites are in degrees starting in the North with 0 degrees, clockwise increasing, ending at 360 degrees in North again. The elevation of the satellites starts at the horizon at 0 degrees, elevating to 90 degrees on top above the observer.

The inclination angle of the satellites planes of GPS and GLONASS is different. GPS has 6 orbital planes at an inclination angle of 55° and GLONASS has 3 orbital planes at an inclination angle about 10 degrees higher than GPS. For an observer, the differences between these factors are shown in figure 4.15.



**Figure 4.15** Skyplots of GPS satellites to the left and GLONASS satellites to the right. Green colour is L1 and L2 and blue colour is satellites transmitting L5 signals. Directions to the satellites from observer in degrees are on the outside of the circle. N is 000° and S is 180°. Elevations in degree from observer to the satellites are inside the circle starting at 0° at the horizon and 90° in zenith above the observer in origin of the plot.

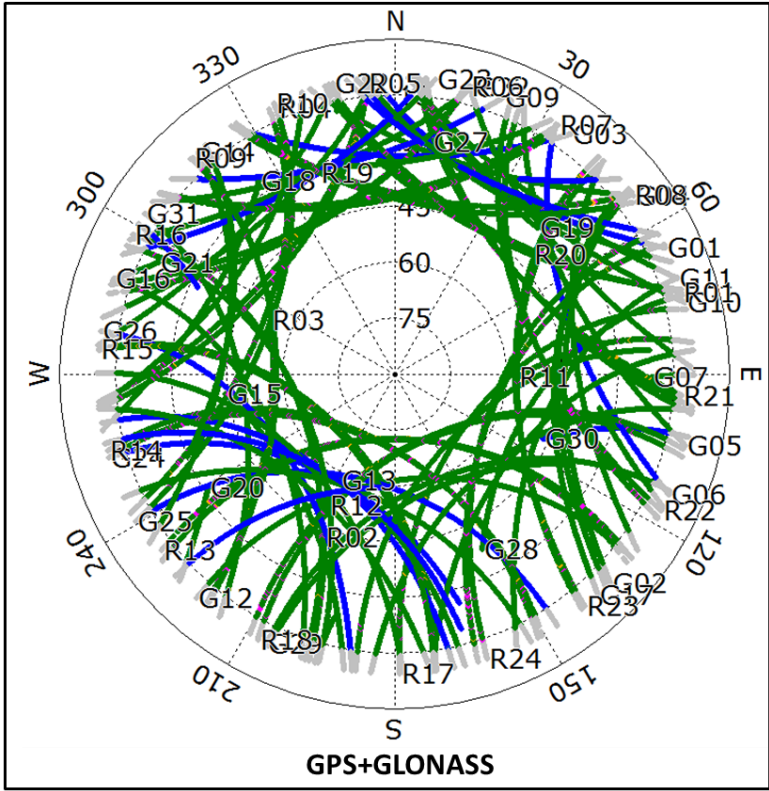
The skyplot of GPS in figure 4.15 has a good density of satellites from the horizon and up to maximum 61 degrees in southern direction and up to about 34 degrees in North. There is a gap in the plot which is not covered by any GPS satellites. At high latitude as in this research the gap hole is above and to the northern direction of the observer. Further south, in Nottingham the gap is in northern direction only. The diameter of the GPS gap is about 42 degrees (not  $90-55=35$ ) as seen from the observer.

The skyplot of GLONASS in figure 4.12 has the satellites spread from the horizon and up to maximum 72 degrees in southern direction which is about 11 degrees higher than GPS. In the North GLONASS satellites reach the elevation of about 45 degrees which is about 11 degrees higher than GPS. The reason for having 11 and not the 10 degrees inclination' difference is the two systems orbital altitudes. The GPS orbital altitude is



about 1.1 km higher altitude than GLONASS satellites altitude. The diameter of the GLONASS gap is about 30 degrees which is about 12 degrees smaller than GPS. Due to that fact that GLONASS satellites are extended over a larger elevation area than GPS, the density of GLONASS satellites is therefore lower than the density of GPS satellites. Lower satellite density may have an effect on the number of satellites in view when the antenna is moving on board a ship.

The assessment in the research hypothesis that GLONASS satellites reach higher altitude from the observer is correct.



**Figure 4.16** Skyplot of the combined GPS+GLONASS satellites

The two systems together in a combined GNSS system have benefits exceeding each of the GPS and GLONASS systems. The numbers of satellites are doubled to 48 operational satellites. The gap of no satellites coverage has the same size and location as GLONASS. The density of satellites is much better than for GPS alone and GLONASS alone.

The GPS+GLONASS combination has the highest density of satellites and this may have an effect of the number of satellites in view when the antennae start moving.

**4.2.4 DOP**

The dilution of precision is an expression of the GNSS satellite constellation geometry.

The average DOP values of the long period are:

Long Period Base Station	DOP (average)		
	GDOP	HDOP	VDOP
GPS	3.2	1.0	2.6
GLONASS	3.8	1.3	3.0
GPS+GLONASS	2.0	0.7	1.6

**Table 4.2** Table of DOP average values of the long period. Green colour represents best DOP value.

Having the skyplot analysis in mind, the GPS with the good spread and density of satellites, the HDOP is very good and VDOP is not as good which gives the GDOP of lower precision than HDOP and VDOP.

GLONASS with lower satellite density than GPS has lower dilution of precision values than GPS.

The GPS+GLONASS combination however, with the high density of satellites, good coverage in altitude and twice the number of satellites has the best DOP in all GDOP, HDOP and VDOP values.

The more satellites in view increase the dilution of precision.

## 4.3 Short Period

### 4.3.1 Accuracy and Precision

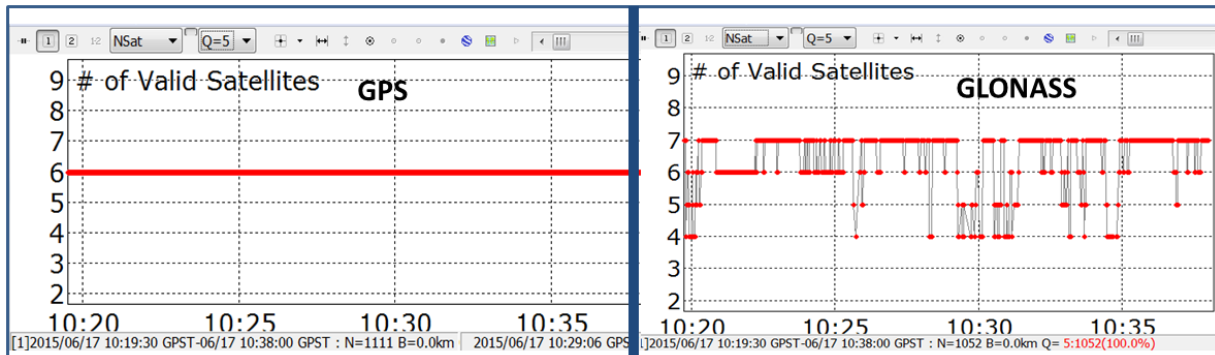
The analysis of accuracy and precision in the short period has emphasis on new discovery not yet discussed in the long period. The same GNSS combinations as in long period have been processed and their absolute accuracy and the precision set into table 4.3.

Short Period Base Station	Accuracy (m)			Precision (std) (m)		
	N	E	U	N	E	U
GPS Single L1	0.63	1.14	11.57	0.59	0.39	3.05
GLONASS	4.15	0.78	7.99	1.50	1.09	4.15
GPS Dual L1+L2	0.6	1.18	1.63	0.51	0.43	2.42
GPS+GLONASS	1.56	0.37	5.15	0.42	0.32	1.94
DGPS	0.05	0.12	0.02	0.27	0.22	1.08

**Table 4.3** The table is the accuracy and precision as performed by the GNSS combinations in the short period at base station.

The aim of the short period is to investigate the GNSS combinations performances in accuracy and precision when both GPS and GLONASS having low number of satellites. All GNSS approaches were recorded at base station. The green colour is the best value in a row and red the worst.

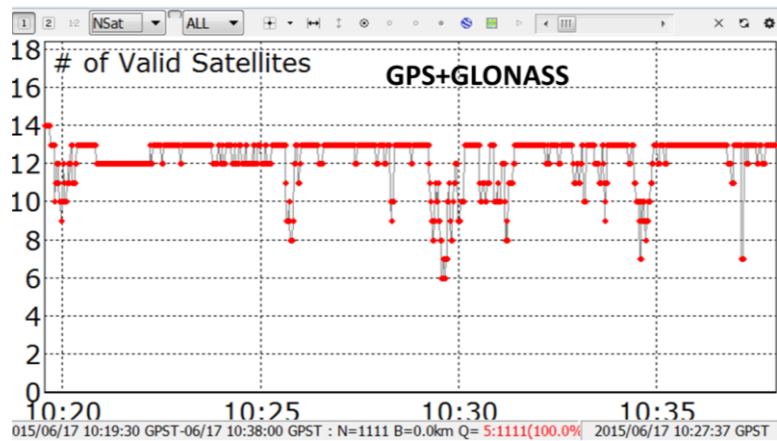
GPS single has about the same values as in long period (table 4.1) in both accuracy and precision in North and Up directions. In the East direction the accuracy compared to table 4.1 has gone down to 1.1m with a better precision. The HDOP is higher in the short period than in the long period and GPS Single has still the lowest accuracy in height. The number of satellites for the GPS combination is stable at 6 satellites.



**Figure 4.17** The number of satellites used in the short period by GPS to the left and GLONASS to the right.

As we can see in figure 4.17 the plots and results of GLONASS continue to be scattered and disturbed. The GLONASS system is in 8 cases down to the limit of minimum 4 satellites to be able to solve a positioning solution. In one epoch (10:29 GPST) GLONASS was not able to solve the position. The accuracy and precision were affected, and GLONASS had in overall the lowest accuracy and precision of the compared GNSS approaches.

GPS Dual had the lowest accuracy in East direction and both GPS Single and GPS Dual had a low accuracy in the East direction.

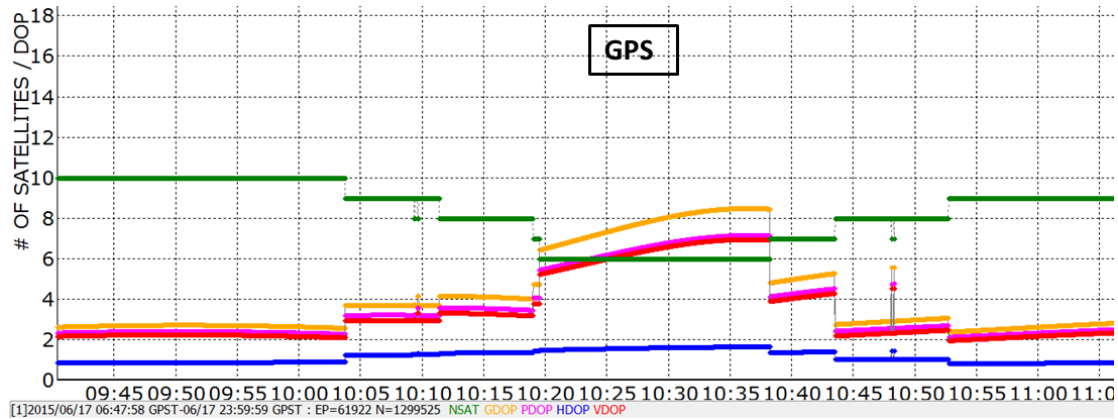


**Figure 4.18** The number of satellites used in the short period by GPS+GLONASS.

GPS+GLONASS however, do not have few satellites to track because both the GPS and GLONASS satellites are available to the receiver (figure 4.18). The reasons discussed in chapter long period still count being advantageous for use in both systems; even more voluminous in situations when each of GPS and GLONASS have few satellites to track. Compared to stand-alone pseudo-range combinations, the combined GPS+GLONASS approach has the best accuracy in East direction and best precision in all North, East and Up. This is achieved in spite of the disturbances on GLONASS system.

### 4.3.2 DOP and Number of Satellites

In the short period the relation between the numbers of satellites in view and DOP values is very clear as shown in figure 4.19.



**Figure 4.19** A plot of GPS DOP values and number of satellites. Yellow colour is GDOP, red is VDOP and blue is HDOP. Green colour is number of satellites.

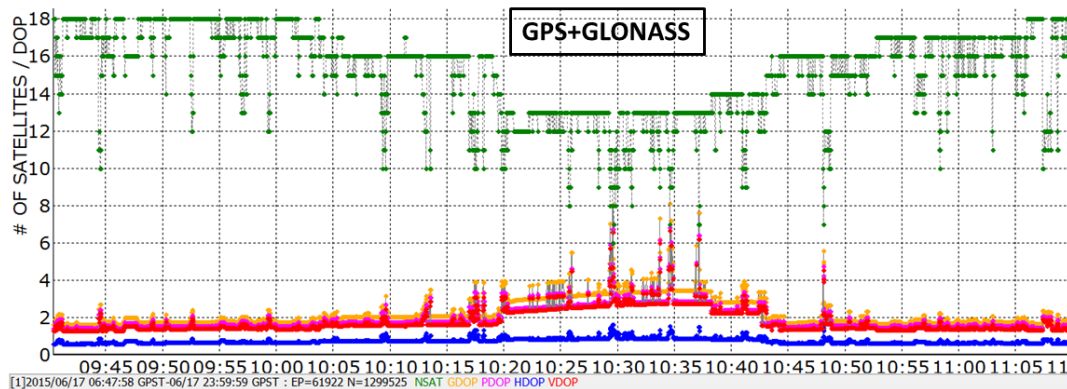
The plot of both GPS DOP values and number of satellites demonstrates their relation.

The GDOP value of about 3 when ten satellites are available is reduced to above 8 when the receiver can use only six satellites. When more satellites are available, the GOP increases to about 3 again.

VDOP is reduced from about 2 to 7. Lack of satellites of high elevation, is the reason for the big change.

HDOP have the same pattern which reduces the HDOP from 1 to 2. Due to the spread of GPS satellites in more horizontal direction, the HDOP is not changing as much as VDOP and GDOP.

The GPS DOP values are affected by a low number of satellites in view.



**Figure 4.20** A plot of GPS+GLONASS DOP values and number of satellites.

The GPS+GLONASS DOP values (figure 4.20) in the same time period as GPS in figure 4.19, tell a quite different story. The changing of HDOP is very small because the available satellites of the GPS+GLONASS receiver are higher. Unlike the GPS receiver, the receiver does not experience the few numbers of satellites.

The GDOP and VDOP change along with the number of satellites but not as much as for GPS. The lowest value of GDOP is only about 3.5 compared to 8. The VDOP value is only about 3 compared to 7.

The DOP of multi GNSS combination benefits in the redundancy of using two GNSS systems instead of one. The hypothesis that increased number of satellites increases the redundancy is correct.

### **4.3.3 Robustness and Redundancy**

According to GSA GNSS market rapport 2015: *"SOLAS' vessels: all passenger ships and cargo ships .....are regulated and rely heavily on GNSS for navigation. At least three devices are typically fitted on vessels for redundancy reasons"* (GSA 2015).

Robustness is defined as: *"..the ability of a computer system to cope with errors during execution"* (The Free Dictionary 2015).

Redundancy is defined as: *"...redundancy is the duplication of critical components or functions of a system with the intention of increasing reliability of the system, usually in the case of a backup or fail-safe"* (The Free Dictionary 2015).

Increased redundancy and reliability also increases the robustness. The critical components or functions which can be duplicated in the GNSS systems are:

- Use of two GNSS systems instead of one. Future GNSS systems will increase this duplication.
- Double the number of satellites available for the user receiver. More in the future.
- Increased satellites density and coverage in elevation
- Increased DOP
- Use four GNSS signals instead of one.
- Increased overall SNR
- Larger use of frequency band
- Increased robustness of unintentional and intentional interference by using more signals and larger use of frequency band
- Increased possibility to reduce the effect of multipath
- Increased accuracy and precision
- Increased number of system control authority. Galileo is purely civilian.
- Increased number of ground segment stations
- Increased robustness for gaining safe navigation position solution 24 hours a day, 7 days a week all year.



There are many benefits of using multi GNSS systems instead of one. It gives seafarers in the Arctic region the opportunity to use two GNSS systems instead of one and thereby it will achieve better robustness and redundancy in navigational safety (Glomsvoll 2014). Like all radio-based services, GPS is subject to interference from both natural and human-made sources. A GPS unit can lose reception in the presence of devices designed for intentional radio jamming. Solar flares can also disrupt GPS equipment. For this reason, the U.S. government strongly encourages all GPS users to maintain backup/alternative positioning, navigation, and timing capabilities (GPS 2015). Recently research in jamming by Glomsvoll has demonstrated that it provides advantages in reliability and redundancy to apply GLONASS system in addition to GPS. The pseudo-range precision has also appeared to be better in combined mode under difficult jamming conditions by the fact that the receiver in combined mode has more satellites to choose from and the better coverage of the GLONASS system, not necessarily because of better jamming resistance for the GLONASS signals (Glomsvoll 2014).

As GLONASS provides more satellites with higher elevation and because it applies a different modulation technique than GPS, the use of both systems would provide better redundancy.

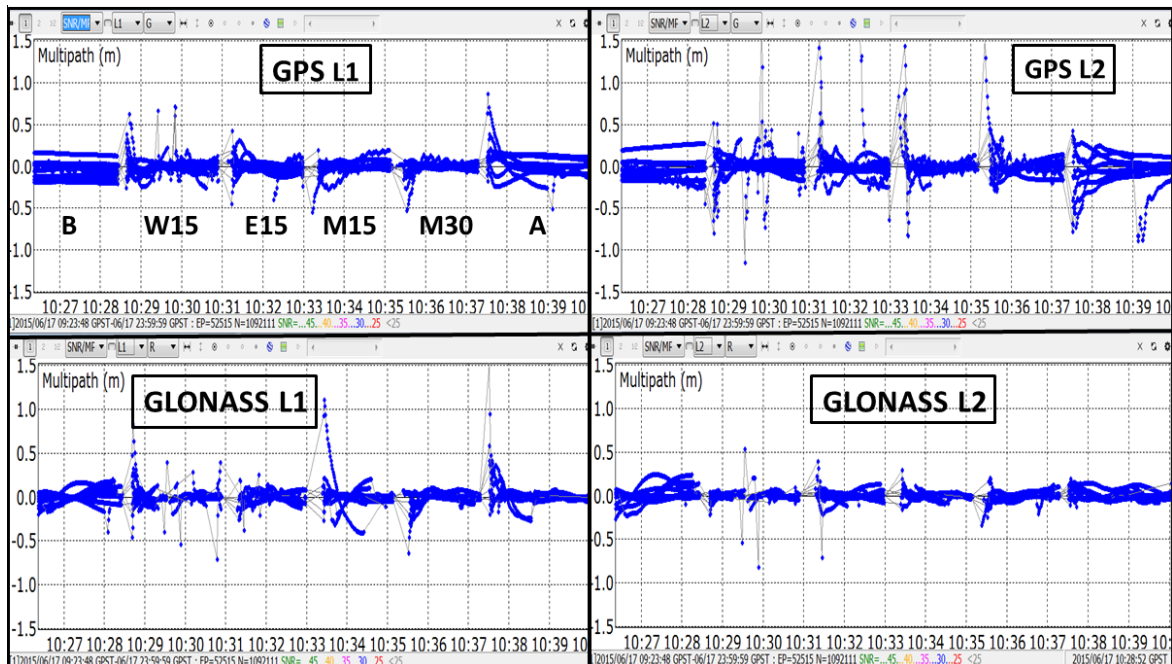
#### **4.4 Ship Movement Simulation**

The analysis of accuracy and precision in the ship movement simulation has emphasis on new discovery. The major difference from static periods is the change in number of satellites caused by the tilt. The multipath conditions around the antenna will change and the view of antenna will see the horizon and the sea below the horizon in the tilted direction.

##### **4.4.1 Multipath Tilt Cycle 2B**

The height of antenna in the research was only 1.4m above the snow and not the 10-30m above the sea as maritime GNSS antennae have on board. The delay caused by

reflection on the snow will be equivalent shorter than reflections caused by the sea on board the ship. The multipath measured during the 2B cycle is shown in figure 4.21.



**Figure 4.21** Plots of multipath from tilt cycle 2B. GPS L1 is upper left, GPS L2 upper right, GLONASS L1 is bottom left and GLONASS L2 is bottom right. X axis is GPST and Y axis is multipath in meter. Tilt cycle 2B is: B=before, W15=tilt west 15 degrees, E15=tilt east 15, M15=moving 15 degrees, M30=moving 30 and A=after.

The gaps in the plots in figure 4.21 are the complete covering of the antenna. The purpose is to separate the different parts of the tilt cycle.

GPS L2 has the largest movements on the plot. It is the most scattered plot with the largest deviations.

GPS L1 has the second largest movements, slightly less than GPS L2.

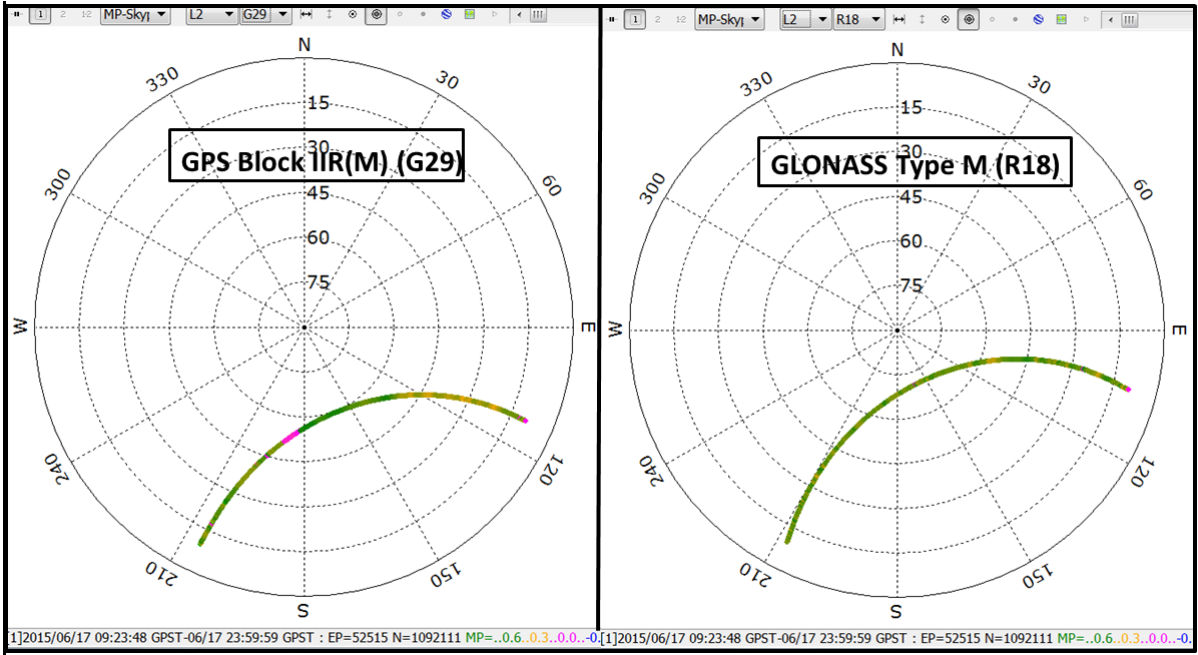
GLONASS L1 is more united on the plot than GPS L1.

GLONASS L2 has the lowest scatter and is most close to 0m multipath.

Different frequencies have different reflection characteristics and are depending of the wavelength. The GLONASS L1 and GPS L1 are close to each other in frequency. The small difference in frequency may have a minor impact on the multipath. The main reason for the different multipath performance is the chipping rate of the C/A code signals. GPS has 1023 kbits/sec and GLONASS has 511 kbits/sec. GLONASS has about twice the chip rate compared to GPS. The maximum theoretical multipath error is one chip length or about 290m for GPS L1 C/A code and about 145m for GLONASS L1.

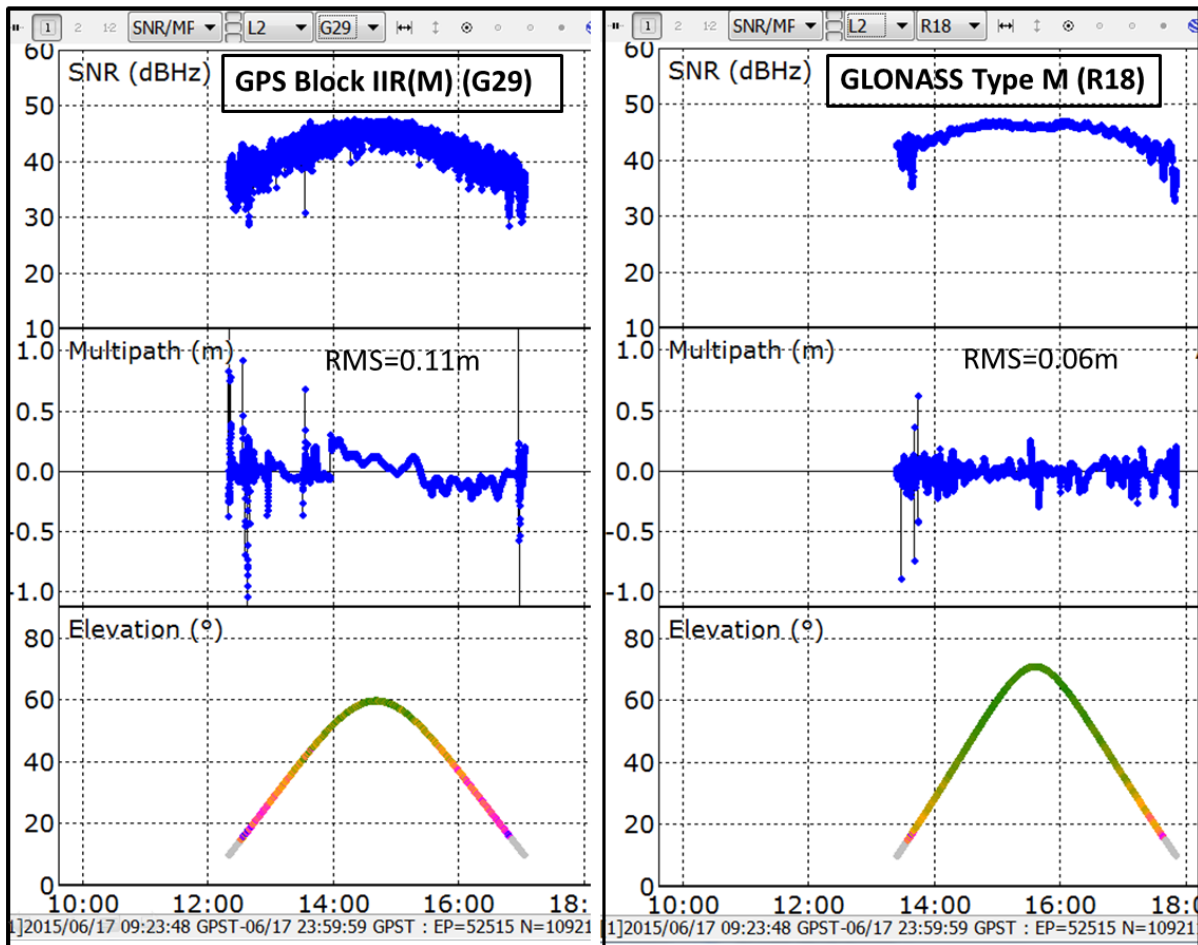
A general comparison of the multipath from research base station is:

- GLONASS L2 has the lowest multipath error
- GLONASS L1 has the second lowest multipath error
- GPS L1 has the third lowest multipath error
- GPS L2 has the highest multipath error



**Figure 4.22** Skyplot of GPS satellite G29 to the left and GLONASS satellite R18 to the right.

The satellites G29 and R18 have about the same elevation, same direction at about the same time. G29 is a Block IIR (M) GPS satellite and R18 is a Type M GLONASS satellite. The G29 and R18 share about the same condition from an observer making the comparison reliable.



**Figure 4.23** Plot of SNR, multipath and elevation in time series of G29 to the left and R18 to the right.

The relation of the satellites elevation impact on both SNR and multipath is clear in both satellites. Low elevation means low SNR and also variable SNR. SNR of G29 starts at about 30 dBHz and has a peak value of about 48 dBHz compared to R18 which starts about 35 and has the peak value of about 47. The mean SNR value of R18 is higher and the distribution is narrower than G29.

G29 has a greater impact on the multipath graph at low elevation and overall about the double value in multipath with RMS at 0.11m compared to RMS 0.06m of the R18.

The highest elevation of G29 is about 60 degrees compared to R18 which culminates at about 71 degrees.

However, due to the higher speed and the planes inclination angle to equator higher than GPS satellites, the R18 has about 15 minutes shorter time in view than G29.

**4.4.2 Accuracy and Precision**

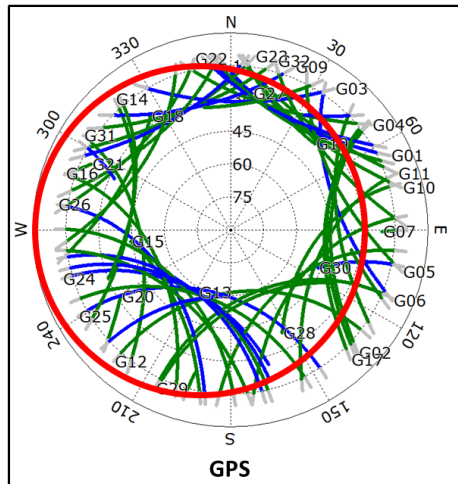
The measurement from tilt cycle 2B on rover antenna is compared to the measurement of the static base station. The GNSS combinations were processed and the results put into tables.

Moving Antenna Cycle 2B GPS Single	Moving Antenna						Base Station (static)					
	Accuracy (m)			Precision (std)			Accuracy (m)			Precision (std)		
	N	E	U	N	E	U	N	E	U	N	E	U
Before	0.2	1.6	9.6	0.8	0.2	0.4	0.2	1.1	9.4	0.1	0.2	0.3
Tilt West 15°	0.7	0.9	12.0	0.1	0.1	0.3	0.8	1.0	11.8	0.2	0.1	0.8
Tilt East 15°	1.3	0.9	14.4	0.1	0.1	0.3	1.2	0.8	13.9	0.1	0.1	0.3
Move 15°	1.7	0.6	20.2	0.3	0.3	1.2	1.3	0.7	15.3	0.1	0.1	0.6
Move 30°	1.4	0.8	16.5	0.1	0.0	0.3	1.3	0.8	15.9	0.1	0.0	0.2
After	1.9	0.8	19.2	0.0	0.0	0.2	1.8	0.9	18.9	0.0	0.0	0.2

**Table 4.4** The table of GPS Single. The tilt moving antenna is to the left and static antenna to the right.

The GPS Single has the largest difference compared to base station when the antenna moved 15 degree back and forth. The reason is the multipath on GPS L1. GPS Single was stable in number of satellites during the tilt cycle. GPS Single was overall less affected by the change in tilt.

The reason of the stable performance of GPS during the ship moving simulation is the stable number of satellites. The change in accuracy and precision is mainly due to the multipath. The high density of GPS satellites at the horizon and above helps the GPS antenna. In the tilting direction, new satellites can be seen at the same rate as the antenna loose satellites at the opposite direction.



**Figure 4.24** Skyplot of the antenna view. The red circle is when the antenna is tilted to west.

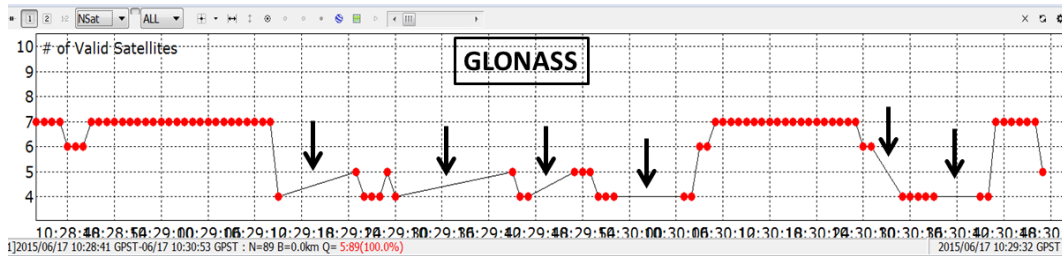
The red circle represents the view of the antenna. When the antenna is moving, the red circle will move and see new satellites at the same rate as satellites are lost on the other side.

Moving Antenna Cycle 2B GLONASS	Moving Antenna						Base Station (static)					
	Accuracy (m)			Precision (std)			Accuracy (m)			Precision (std)		
	N	E	U	N	E	U	N	E	U	N	E	U
Before	3.7	0.6	5.9	0.6	0.5	1.6	3.9	0.5	5.8	1.1	0.7	2.3
Tilt West 15°	5.5	1.8	11.3	2.2	1.4	3.6	5.7	1.9	10.9	2.6	1.7	4.4
Tilt East 15°	3.0	1.4	3.4	0.8	1.0	4.5	3.9	1.0	7.2	1.5	1.1	4.5
Move 15°	4.4	1.4	9.6	2.3	1.5	5.9	4.2	0.9	10.2	1.6	1.3	6.5
Move 30°	4.0	0.2	8.8	0.7	0.6	4.6	3.7	0.1	7.9	0.4	0.3	3.7
After	3.7	0.6	7.0	0.5	0.4	1.5	4.1	0.4	7.1	1.9	0.7	2.9

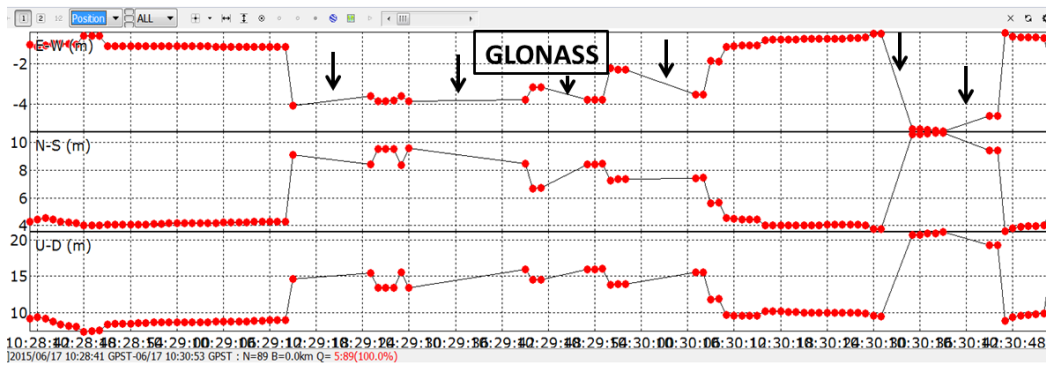
**Table 4.5** The table of GLONASS. The tilt moving antenna is to the left and static antenna to the right.

The GLONASS system was down to the limit of four satellites in the static short period. The table 4.5 show the average values during the moving period and not the lost epochs. GLONASS was largely affected by the antenna tilt movements and was not able to solve

position solutions for six periods. The gaps where the numbers of GLONASS satellites were below 4 are shown in figure 4.25. The gaps in epoch positions are shown in figure 4.26.



**Figure 4.25** Plot of GLONASS number of satellites. The six periods where the numbers of GLONASS satellites were below 4 are marked with an arrow.



**Figure 4.26** Plot of GLONASS position. East-West is the top plot. North-South is the middle plot and Up-Down is the bottom plot. The six periods where GLONASS were not able to solve positions are marked with an arrow.

The density of GLONASS satellites is less than for GPS. The tilted antenna may not replace a lost satellite on one side at the same rate as it gets a new satellite one on the other side. The GLONASS plots are still distorted. The combination of a tilting antenna and the challenge of acquire and track the GLONASS signals, may be the reason for not be able to calculate position solution. GLONASS system was unreliable during this part of the research.



Moving Antenna Cycle 2B GPS Dual	Moving Antenna						Base Station (static)					
	Accuracy (m)			Precision (std)			Accuracy (m)			Precision (std)		
	N	E	U	N	E	U	N	E	U	N	E	U
Before	0.2	1.3	0.4	0.1	0.2	0.4	0.3	1.1	0.2	0.1	0.1	0.4
Tilt West 15°	0.7	0.9	2.1	0.1	0.1	0.3	0.6	1.0	1.7	0.2	0.1	0.7
Tilt East 15°	1.1	0.9	4.2	0.1	0.1	0.3	1.1	0.8	3.6	0.1	0.1	0.2
Move 15°	1.3	0.6	5.6	0.1	0.1	0.8	1.2	0.7	4.6	0.1	0.1	0.5
Move 30°	1.2	0.8	5.6	0.1	0.1	0.4	1.2	0.8	5.1	0.1	0.1	0.2
After	0.9	1.0	2.7	0.1	0.1	0.1	0.9	1.1	2.3	0.1	0.1	0.1

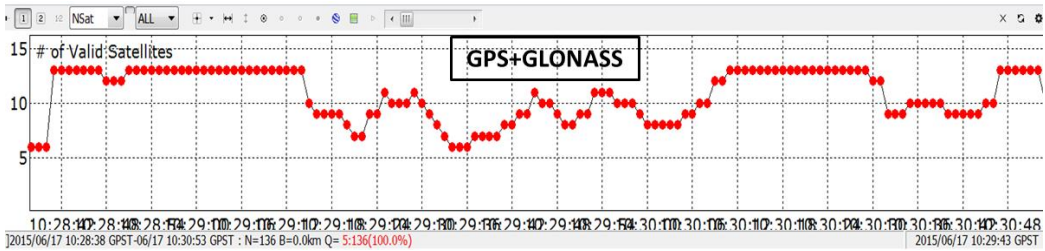
**Table 4.6** The table of GPS Dual. The tilt moving antenna is to the left and static antenna to the right.

GPS Dual was able to use six satellites during the moving period. The differences in accuracy and precision between the rover antenna and the station antenna are overall small. GPS Dual is reliable of solving position solution when the antenna moves in tilt. The combination has the best performance in accuracy and precision of the pseudo-range combinations.

Moving Antenna Cycle 2B GPS+GLONASS	Moving Antenna						Base Station (static)					
	Accuracy (m)			Precision (std)			Accuracy (m)			Precision (std)		
	N	E	U	N	E	U	N	E	U	N	E	U
Before	1.1	0.4	3.4	0.2	0.2	0.9	1.2	0.4	3.4	0.3	0.2	1.1
Tilt West 15°	1.5	0.4	5.4	0.4	0.5	1.4	1.5	0.4	4.6	0.4	0.4	1.5
Tilt East 15°	1.9	0.1	5.7	0.3	0.5	1.1	1.9	0.1	6.1	0.3	0.2	1.8
Move 15°	1.9	0.1	7.0	0.5	0.4	1.8	1.8	0.2	7.1	0.3	0.3	1.6
Move 30°	2.0	0.3	7.7	0.1	0.1	0.9	1.9	0.4	7.6	0.2	0.1	1.0
After	1.5	0.8	4.4	0.3	0.2	1.1	1.6	0.8	3.9	0.2	0.1	0.7

**Table 4.7** The table of GPS+GLONASS. The tilt moving antenna is to the left and static antenna to the right.

The combined GPS+GLONASS can exploit the number of GPS satellites and the lower multipath error from the GLONASS signals.



**Figure 4.27** The plot of GPS+GLONASS satellites.

The numbers of available satellites are high although the GLONASS system had epoch gaps. Compared to GPS, the numbers of satellites were higher except in six epochs when it was equal number. There are overall small differences in accuracy and precision between the rover antenna and the station antenna. GPS+GLONASS combination is reliable of solving position solution when the antenna moves in tilt. The overall accuracy and precision is better than the GLONASS and GPS Single but slightly below the GPS Dual.

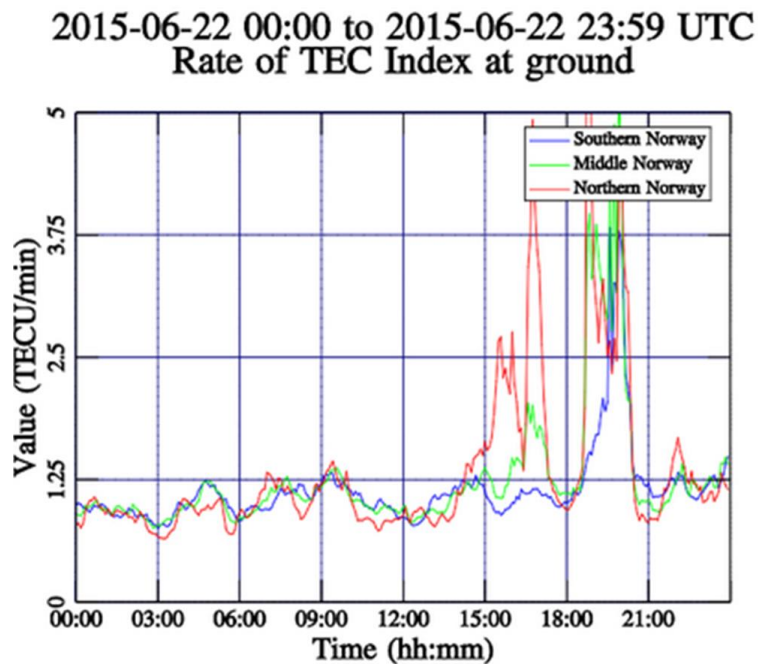
Moving Antenna Cycle 2B DGPS	Moving Antenna						Base Station (static)					
	Accuracy (m)			Precision (std)			Accuracy (m)			Precision (std)		
	N	E	U	N	E	U	N	E	U	N	E	U
Before	0.0	0.0	0.1	0.0	0.0	0.0	0.0	0.0	0.1	0.0	0.0	0.0
Tilt West 15°	0.0	0.3	0.3	0.0	0.0	0.1	0.1	0.3	0.1	0.3	0.2	0.5
Tilt East 15°	0.2	0.0	0.7	0.1	0.1	0.3	0.2	0.3	0.2	0.9	0.7	0.4
Move 15°	0.2	0.2	0.8	0.1	0.1	0.5	0.1	0.2	0.7	0.1	0.1	0.4
Move 30°	0.0	0.1	0.7	0.1	0.1	0.5	0.1	0.1	0.0	0.3	0.2	1.7
After	0.1	0.0	0.7	0.0	0.0	0.0	0.0	0.0	0.7	0.0	0.0	0.0

**Table 4.8** The table of DGPS. The tilt moving antenna is to the left and static antenna to the right.

DGPS maintained high accuracy and precision during the ship simulation and benefits of the stable number of GPS satellites. The combination has the best overall performance in accuracy and precision in the ship moving simulation test.

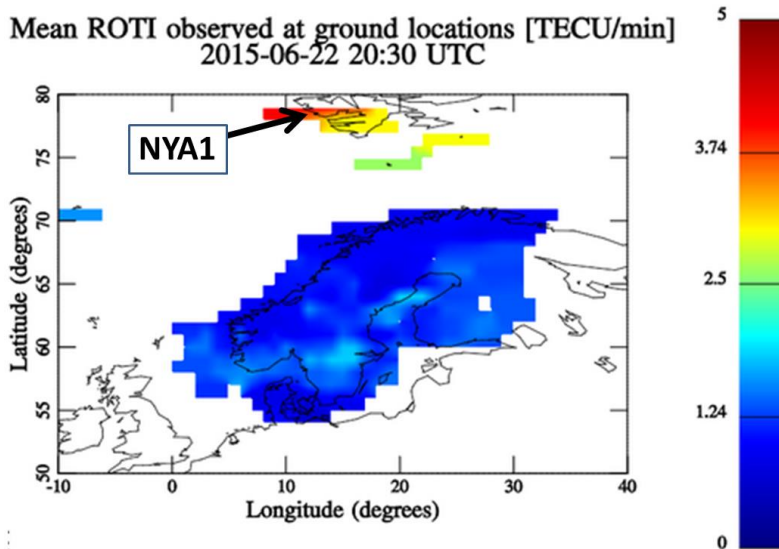
## 4.5 Sun Activity NYA1

There was sun activity from about 15:00 to 20:30 on 22 June 2015.



**Figure 4.28** Plot of the Rate of TEC Index at ground in Norwegian territory. Northern Norway (and Svalbard) is the red line (Kartverket 2015).

To investigate when the TEC was high at NYA1 in Svalbard the simulator in Kartverket, was used. Most of the high TEC on ground was further south, but the largest TEC found was a short period at 20:30 on 22 June 2015 (figure 4.28) (Kartverket 2015).



**Figure 4.29** Plot of the mean ROTI (TECU/min) in Norwegian territory and NYA1.

Data recorded at NYA1 Reference Station was processed using the GPS Single and GPS+GLONASS combinations. The results of sun activity from 20:27 to 20:32 are compared to the closest normal period from 20:52 to 20:57.

Sun Activity NYA1 Reference Station	Sun Activity						Normal					
	Accuracy (m)			Precision (std)			Accuracy (m)			Precision (std)		
	N	E	U	N	E	U	N	E	U	N	E	U
GPS Single	1.8	0.3	9.7	0.3	0.2	0.7	1.3	0.2	13.8	0.1	0.1	0.4
GPS+GLONASS	1.4	0.3	2.0	0.3	0.3	0.9	0.8	0.1	0.9	0.2	1.1	0.4

**Table 4.9** A table of the sun activity which occurred on 22 June. The sun activity is displayed to the left and a normal period to the right of the table.

The accuracy plots of both sun activity and normal period were normal. The GPS+GLONASS combination had the best overall accuracy and precision in both periods. None missed epochs or irregular changes in the valid number of satellites or pseudo-ranges residuals were observed. None reduced strength in SNR was observed, either in the GPS or GLONASS satellites' signals.

Scintillations are ionospheric effects which affect GNSS signals. Scintillations are rapid fluctuations in the amplitude and phase of the signals caused by small-scale irregularities in the ionosphere. When sufficiently strong, scintillations can result in the strength of a received signal dropping below the threshold required for acquisition and tracking. According to Langley, the scintillations at high latitude were more frequent during night-time. In high latitude, the scintillations follow a half-year cycle (Langley 2015).

The arctic area around Svalbard and NEP is in the aurora borealis area and the seasonal cycle and diurnal cycle are special at this high latitude. The season when the majority of civilian vessels use the NEP area is from June to October when there is midnight sun and day conditions occur 24 hours a day or short nights (October).

NYA1 reported total number of 100 cycle slips during the 24 hours on 22 June 2015 (IGS 2015).

Both GPS Single and GPS+GLONASS approaches conducted position solution as normal during the sun activity around 20:30 on 22 June 2015.

## **5 CONCLUSION**

All the GNSS combinations used in the research fulfil the GPS Standard Positioning Service Performance Standard of the minimum pseudo-range accuracy of 7.8 meters at a 95% confidence level, and the Maritime Safety Committee 95, International Maritime Organisation's Performance Standard.

GLONASS had the lowest overall accuracy and precision and was affected most in the ship moving simulation.

GPS Single frequency has higher overall accuracy and precision than GLONASS, but was affected by the ionospheric delay.

GPS Dual frequency performed better than GPS Single and GLONASS due to the possibility of removing the ionospheric bias.

DGPS has the best performance in accuracy and precision but limited area in NEP makes it difficult to exploit the benefits of DGPS.

GNSS receivers can be affected by sun activity. Both GPS Single and GPS+GLONASS approaches were not affected by the sun activity during the research periods on 22 June 2015.

GPS+GLONASS combination was able to: exploit both GPS and GLONASS systems, all their satellites, all available civil signals, able to mask signals hampered by multipath or low altitude, use satellite constellation with high HDOP and VDOP and performed the most overall reliable good quality positioning solutions.

The GPS+GLONASS combination has shown to be more robust in accuracy, precision, availability of all GNSS satellites and their signals during the static and dynamic test in the Arctic. Due to redundancy and robustness, it is advantageous to use the GPS+GLONASS combination for safe navigation in the arctic area around Svalbard and in the Northeast Passage for civilian vessels.

## 6 RECOMMENDATIONS

All the GNSS combinations; GPS Single using L1 only, GLONASS, GPS Dual using L1 and L2, combined GPS+GLONASS and DGPS can be used in the arctic area around Svalbard and in the NEP.

More multi GNSS Reference Stations are needed in NEP to be able to exploit DGNSS in coastal and harbour areas.

It is important to stress the value of maintaining the classic navigational methods such as radar navigation and terrestrial navigation in coastal waters and not alone depend on GNSS.

It is advantageous to use the GPS+GLONASS combination for safe navigation in the arctic area around Svalbard and in the Northeast Passage for civilian vessels due to the redundancy of the GPS and GLONASS systems.

If you aboard your vessel prioritize robustness to ensure high quality positional solutions in accuracy and precision, coverage and density of satellites, utilizing all available satellite signals and better equipped to deal with interference?

-Multi-constellation GNSS equipment is your answer!



**Figure 6.1** Polar bear at Svalbard (adopted from Norsk Polarinstitut)



## REFERENCES

- Bingley, R. (2014), *Handouts Satellite Based Positioning (H24VST)*, The University of Nottingham, Nottingham, UK.
- Braw, E. (2015), *Prospects for the Northeast Passage* [Online] Retrieved from: <http://www.worldaffairsjournal.org/blog/elisabeth-brow/prospects-northeast-passage> on 4 August 2015
- Buixadè, F., Stephenson, S R., Chen, L., Czub, M., Dai, Y., Solski, J. (2014), 'Commercial Arctic shipping through the Northeast Passage: routes, resources, governance, technology, and infrastructure', *Polar Geography*, **37**(4): pp 298-324
- Davis, M. (2011), *Study skills for international postgrads*, New York, USA: Palgrave Study Skills.
- EGNOS (2015), *About EGNOS - What is SBAS?* [Online] Retrieved from: <http://egnos-portal.gsa.europa.eu/discover-egnos/about-egnos/what-sbas> on 7 August 2015
- Elmas, Z G. (2013), *Exploiting New GNSS Signals to Monitor, Model and Mitigate the Ionospheric Effects in GNSS*. Ph.D. dissertation, Nottingham Geospatial Institute, The University of Nottingham, Nottingham, UK.
- GPS (2015), *GPS Accuracy* [Online] Retrieved from: <http://www.gps.gov/systems/gps/performance/accuracy/> on 18 August 2015
- GPS (2015), *Space segment* [Online] Retrieved from: <http://www.gps.gov/systems/gps/space/> on 2 August 2015
- GPS (2015), *Jamming* [Online] Retrieved from: <http://www.gps.gov/support/faq/#jamming> on 2 August 2015
- Glomsvoll, O. (2014), *Jamming of GPS & GLONASS Signals. A study of GPS performance in maritime environments under jamming conditions, and benefits of applying GLONASS in Northern areas under such conditions*. MSc. Nottingham Geospatial Institute, The University of Nottingham, Nottingham, UK.
- GLONASS IAC (2015), *Information-Analytical Centre –GLONASS Status* [Online] Retrieved from: <https://glonass-iac.ru/en/GLONASS/> on 20 August 2015
- GNSS Pro (2015), *IALA DGPS Reference stations* [Online] Retrieved from: <http://www.gnsspro.com/referencestations.php> on 7 August 2015
- GPS World (2015), *Orbit Data and Resources on Active GNSS Satellites* [Online] Retrieved from: [http://gpsworld.com/wp-content/uploads/2015/01/GPS\\_World\\_Almanac\\_Jan2015.pdf](http://gpsworld.com/wp-content/uploads/2015/01/GPS_World_Almanac_Jan2015.pdf) on 9 August 2015

- GPS World (2015), *Reference station* [Online] Retrieved from: <http://gpsworld.com/tag/reference-station> on 20 February 2015
- Groves, P. (2013), *GNSS, Inertial, and Multisensor Integrated Navigation Systems*. Boston, London, UK: Artech House.
- GSA (2015), *GNSS Market Report Issue 4 2015* [Online] Retrieved from: [http://www.gsa.europa.eu/sites/default/files/Maritime\\_0.pdf](http://www.gsa.europa.eu/sites/default/files/Maritime_0.pdf) on 7 August 2015
- IGS (2015), *Station Details* [Online] Retrieved from: <http://www.igs.bkg.bund.de/station/list> on 20 July 2015
- IEEE Explore (2014), *Figures* [Online] Retrieved from: [http://ieeexplore.ieee.org/ieee\\_pilot/articles/96jproc12/jproc-CHegarty-2006090/article.html](http://ieeexplore.ieee.org/ieee_pilot/articles/96jproc12/jproc-CHegarty-2006090/article.html) on 2 December 2014
- Inside GNSS (2014), *Measuring GNSS Signal Strength* [Online] Retrieved from: [www.insidegnss.com/node/2397](http://www.insidegnss.com/node/2397) on 4 December 2014
- IMO (2015), *(NCSR), 2<sup>nd</sup> session, 9-13 March, 2015* [Online] Retrieved from: <http://www.imo.org/en/mediacentre/meetingsummaries/NCSR/Pages/NCSR-2nd-session.aspx> on 18 August 2015
- Kaplan, E. and Hegarty, C. (2006), *Understanding GPS. Principles and applications*. Norwood, MA: Artech House.
- Kartverket (2015), *Kartverket* [Online] Retrieved from: [www.kartverket.no](http://www.kartverket.no) on 5 July 2015
- KSAT (2015), *KSAT – Satellite Service* [Online] Retrieved from: [www.KSAT.no](http://www.KSAT.no) on 6 June 2015
- Langley, R B. (2007), 'Propagation of the GPS signal', *Earth Science*, Vol. **60**: pp 103-140.
- Langley, R B., Taylor, S., Pelgrum, W. (2014), *Innovation: scintillating statistics: A Look at High-Latitude and Equatorial Ionospheric Disturbances of GPS Signals* [Online] Retrieved from: <http://gpsworld.com/innovation-scintillating-statistics/> on 7 August 2015
- Langley, R B (1999), 'Dilution of Precision', *GPS World*, 1999: pp 52-59.
- Leick, A., Rapoport, L., Tatarnikov, D. (2015), *GPS Satellite Surveying*. Hoboken, New Jersey, USA: John Wiley & Sons, Inc.

- Meng, X. (2002), *Real-time Deformation Monitoring of Bridges Using GPS/Accelerometers*. Ph.D. dissertation, Institute of Engineering Surveying and Space Geodesy, The University of Nottingham, Nottingham, UK.
- Meng, X., Roberts, G W., Dodson, A H., Cosser, E., Barnes, J., Rizos, C. (2004), 'Impact of GPS satellite and pseudolite geometry on structural deformation monitoring: analytical and empirical studies', *Journal of Geodesy* **77**(12): pp 809-822
- Misra, P., Enge, P. (2006), *Global Positioning System. Signals, Measurements, and performance*. Lincoln, Massachusetts, USA: Ganga-Jamuna Press.
- Moore, T. (2015), Lectures and Handouts in Location Technology (H24VLT), The University of Nottingham, Nottingham, UK.
- National Snow and Ice Data Centre (2015), *Arctic Sea Ice News and analysis* [Online] Retrieved from: <http://nsidc.org/arcticseaicenews/> on 8 July 2015
- NAVIPEDIA (2015), *GLONASS Future and Evolution*[Online] Retrieved from: [http://www.navipedia.net/index.php/GLONASS\\_Future\\_and\\_Evolutions](http://www.navipedia.net/index.php/GLONASS_Future_and_Evolutions) on 21 August 2015
- NAVIPEDIA (2015) *Receiver noise* [Online] Retrieved from: [http://www.navipedia.net/index.php/Receiver\\_noise](http://www.navipedia.net/index.php/Receiver_noise) on 22 August 2015
- RTKLIB (2015), *RTKLIB ver. 2.4.2 Manual* [Online] Retrieved from: [http://www.rtklib.com/prog/manual\\_2.4.2.pdf](http://www.rtklib.com/prog/manual_2.4.2.pdf) on 27 June 2015
- Smith, M. (2014), Lectures and Handouts in Least squares, The University of Nottingham, Nottingham, UK.
- Swann, J W. (1999), *Advantages and Problems of combining GPS with GLONASS*. Ph.D. dissertation, Institute of Engineering Surveying and Space Geodesy, The University of Nottingham, Nottingham, UK.
- Sumner, T. (2015), *Iceless Arctic summers now expected by 2050s* [Online] Retrieved from <https://www.sciencenews.org/article/iceless-arctic-summer-now-expected-2015s> on 4 August 2015
- The Free Dictionary (2015), *Robustness* [Online] Retrieved from <http://www.thefreedictionary.com/robustness> on 27 August 2015
- Trimble (2015), *GNSS Planning Online*. [Online] Retrieved from: <https://www.trimble.com/GNSSPlanningOnline/> on 20 February 2015
- Volpe, J. (2001), *Vulnerability assessment of the transportation infrastructure relying on the Global Positioning System*. National Transportation Systems Center, Final report.

Østreng, W. (2010), *The Northeast Passage and Northern Sea Route 2* [Online] Retrieved from: <http://www.arctis-search.com/The+Northeast+Passage+and+Northern+Sea+Route+2> on 6 July 2015

# APPENDICES

## Appendix A: Specifications Leica GS10

### Leica Viva GS10

<b>GNSS PERFORMANCE</b>		
GNSS technology	Leica SmartTrack	Advanced four constellation tracking
Number of channels		120 (up to 60 satellites simultaneously on two frequencies) / 500+ <sup>1</sup>
Signal tracking		GPS (L1, L2, L2C, L5), Glonass (L1, L2), BeiDou (B1, B2), Galileo (E1, E5a, E5b, Alt-BOC), QZSS (L1, L2, L5) <sup>2</sup> , SBAS (WAAS, EGNOS, MSAS, CAGAN)
GNSS antenna	Standard or Choke-ring	Leica AS10 / AS05 or Leica AR10 / AR20 / AR25
<b>MEASUREMENT PERFORMANCE &amp; ACCURACY<sup>3</sup></b>		
RTK technology	Leica SmartCheck Network RTK Time for initialisation	Continuous check of RTK solution, reliability 99.99% VRS, FKP, iMAX, MAC (RTCM SC 104) Typically 4s
Code differential	DGPS / RTCM	Typically 25cm
Real-time kinematic	Single baseline (< 30km) Network RTK	H <sub>z</sub> 8mm + 1ppm / V 15mm + 1ppm H <sub>z</sub> 8mm + 0.5ppm / V 15mm + 0.5ppm
Post processing	Static (phase) with long observations Static and rapid static (phase)	H <sub>z</sub> 3mm + 0.1ppm / V 3.5mm + 0.4ppm H <sub>z</sub> 3mm + 0.5ppm / V 5mm + 0.5ppm
<b>COMMUNICATIONS</b>		
Communication ports	Lemo Bluetooth®	1 x USB and 2 x RS232 serial and Power Bluetooth® v2.00 + EDR, class 2
Communication protocols	RTK data protocols NMEA output	Leica, Leica 4G, CMR, CMR+, RTCM 2.2, 2.3, 3.0, 3.1, 3.2 MSM NMEA 0183 V 4.00 and Leica proprietary
External data links	Up to 3 simultaneously	GSM / GPRS / UMTS / CDMA and UHF / VHF modem / Phone / Radio modem in Leica GFU housing (IP67)
<b>GENERAL</b>		
User interface	Buttons and LEDs Web server	On/Off and Function button, 8 status LEDs Full status information and configuration options
Data recording	Storage Data type and recording rate	Removable SD card, 1 GB Leica GNSS raw data and RINEX data up to 20 Hz
Power management	Internal power supply External power supply Operation time <sup>4</sup>	2 exchangeable Li-Ion batteries (6 Ah / 7.4 V) Nominal 12 V DC, range 10.5 - 28 V DC 15 h receiving RTK data with UHF radio 13 h transmitting RTK data with UHF radio (1W) 14 h receiving / transmitting RTK data with phone modem
Weight and Dimensions	Weight Dimensions	1.20kg (GS10) / 5.40kg standard RTK rover setup using pole and backpack 212mm x 166mm x 79mm
Environmental	Temperature Drop Proof against water, sand and dust  Vibration  Humidity  Functional shock	-40 to 65°C operating, -40 to 80°C storage Withstands topple over from a 2m survey pole onto hard surfaces IP68 (IEC60529 / MIL-STD 810G 506.5 I / MIL-STD 810G 510.5 I / MIL-STD 810G 512.5 I)  Withstands strong vibration (ISO9022-36-08 / MIL-STD 810G 514.6 Cat.24) 100% (ISO9022-13-06 / ISO9022-12-04 / MIL-STD 810G 507.5 I) 40g / 15 to 23 msec (MIL-STD 810G 516.6 I)

LEICA GS10 GNSS RECEIVER	Single Frequency	Performance	Professional	Unlimited <sup>1</sup>
<b>SUPPORTED GNSS SYSTEMS</b>				
GPS L2 / GPS L5 / GLONASS / Galileo / BeiDou	• / • / • / • / •	✓ / • / • / • / •	✓ / ✓ / ✓ / ✓ / •	✓ / ✓ / ✓ / ✓ / ✓
<b>RTK PERFORMANCE</b>				
DGPS/RTCM, RTK Unlimited, Network RTK	•	✓	✓	✓
SmartLink (L-band)	•	•	•	✓
<b>POSITION UPDATE &amp; DATA RECORDING</b>				
5 Hz / 20 Hz positioning	✓ / •	✓ / ✓	✓ / ✓	✓ / ✓
Raw data / RINEX data logging	✓ / •	✓ / •	✓ / ✓	✓ / ✓
NMEA out	•	•	✓	✓
<b>ADDITIONAL FEATURES</b>				
RTK reference station functionality	•	✓	✓	✓
			✓ Standard	• Optional

<sup>1</sup> The Unlimited series includes a future upgrade to 500+ channels.

<sup>2</sup> Support of QZSS is incorporated and will be provided through future firmware upgrade.

The Bluetooth® trademarks are owned by Bluetooth SIG, Inc. Illustrations, descriptions and technical data are not binding. All rights reserved. Printed in Switzerland – Copyright Leica Geosystems AG, Heerbrugg, Switzerland, 2015. 774162en - 05.15 - INT

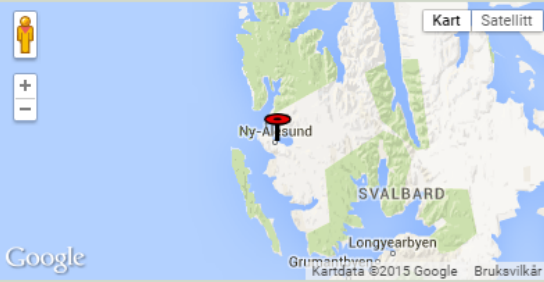
<sup>3</sup> Measurement precision, accuracy, reliability and time for initialisation are dependent upon various factors including number of satellites, observation time, atmospheric conditions, multipath etc. Figures quoted assume normal to favourable conditions. A full BeiDou and Galileo constellation will further increase measurement performance and accuracy.

<sup>4</sup> Might vary with temperature, age of battery, transmit power of data link device.

## Appendix B: Specifications Trimble NETR8

### Station Details

#### Station: NYA1 - Ny-Alesund

General Information	
Projects	IGS EUREF
storedIn	IGS
Date Prepared	29.01.2015 00:00:00
Name	Ny-Alesund
FourCharacterId	NYA1
Maps	 A Google Maps screenshot showing the location of Ny-Alesund on the island of Svalbard, Norway. The map includes a red pin at Ny-Alesund, a person icon, zoom controls, and map style options (Kart, Satellitt). Labels on the map include 'Ny-Alesund', 'SVALBARD', 'Longyearbyen', and 'Grimmanthveng'. The Google logo and copyright information 'Kartdata ©2015 Google Bruksvilkår' are also visible.
DomesNumber	10317M003
Country	Norway
TectonicPlate	EURASIAN
XCoordinate	1202434.0000
YCoordinate	252632.0000
ZCoordinate	6237772.0000
Email	satref@kartverket.no; vlbi@kartverket.no
	Go
Logfile Data	Click <a href="#">here</a> to see the logfile data

Sensors																			
Receiver	<table border="1"> <thead> <tr> <th colspan="2">active Receiver:</th> </tr> </thead> <tbody> <tr> <td>ReceiverType:</td> <td>TRIMBLE NETR8</td> </tr> <tr> <td>SerialNumber:</td> <td>4843K33429</td> </tr> <tr> <td>DateInstalled:</td> <td>29.01.2015 17:00:00</td> </tr> <tr> <td>DateRemoved:</td> <td>NA,NA,NA NA:NA:NA</td> </tr> <tr> <td>SatelliteSystem:</td> <td>GPS+GLO</td> </tr> <tr> <td>FirmwareVersion:</td> <td>4.41</td> </tr> <tr> <td>ElevationCutoffSetting:</td> <td>0 deg</td> </tr> </tbody> </table>	active Receiver:		ReceiverType:	TRIMBLE NETR8	SerialNumber:	4843K33429	DateInstalled:	29.01.2015 17:00:00	DateRemoved:	NA,NA,NA NA:NA:NA	SatelliteSystem:	GPS+GLO	FirmwareVersion:	4.41	ElevationCutoffSetting:	0 deg		
	active Receiver:																		
	ReceiverType:	TRIMBLE NETR8																	
	SerialNumber:	4843K33429																	
	DateInstalled:	29.01.2015 17:00:00																	
	DateRemoved:	NA,NA,NA NA:NA:NA																	
	SatelliteSystem:	GPS+GLO																	
	FirmwareVersion:	4.41																	
	ElevationCutoffSetting:	0 deg																	
	show/hide older receiver																		
Antenna	<table border="1"> <thead> <tr> <th colspan="2">active Antenna:</th> </tr> </thead> <tbody> <tr> <td>AntennaType:</td> <td>ASH701073.1</td> </tr> <tr> <td>SerialNumber:</td> <td>CRG0117</td> </tr> <tr> <td>DateInstalled:</td> <td>02.06.1999 00:40:00</td> </tr> <tr> <td>DateRemoved:</td> <td>NA,NA,NA NA:NA:NA</td> </tr> <tr> <td>MarkerARPUppEcc:</td> <td>0.0000</td> </tr> <tr> <td>MarkerARPNorthEcc:</td> <td>0.0000</td> </tr> <tr> <td>MarkerARPEastEcc:</td> <td>0.0000</td> </tr> <tr> <td>AntennaRadomeType:</td> <td>SNOW</td> </tr> </tbody> </table>	active Antenna:		AntennaType:	ASH701073.1	SerialNumber:	CRG0117	DateInstalled:	02.06.1999 00:40:00	DateRemoved:	NA,NA,NA NA:NA:NA	MarkerARPUppEcc:	0.0000	MarkerARPNorthEcc:	0.0000	MarkerARPEastEcc:	0.0000	AntennaRadomeType:	SNOW
	active Antenna:																		
	AntennaType:	ASH701073.1																	
	SerialNumber:	CRG0117																	
	DateInstalled:	02.06.1999 00:40:00																	
	DateRemoved:	NA,NA,NA NA:NA:NA																	
	MarkerARPUppEcc:	0.0000																	
	MarkerARPNorthEcc:	0.0000																	
	MarkerARPEastEcc:	0.0000																	
	AntennaRadomeType:	SNOW																	
show/hide older antennas																			
Humidity Sensor	no sensor installed																		
Pressure Sensor	no sensor installed																		
Temperature Sensor	no sensor installed																		
Water Vapor Radiometer	no sensor installed																		